

~keV 暗黒物質 by 宇宙観測 & AXION実験

Astronomical searches of dark matter &
microcalorimeter ground experiments

満田和久, JAXA宇宙研

Kazuhisa MITSUDA, ISAS, JAXA

ダークマターの懇談会2019

5-6 July 2019, at Waseda Univ.

Outline

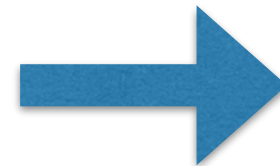
- Story of the 3.5 keV line, and astronomical searches of keV dark matter
 - Sterile neutrinos
 - Where to observe?
 - 3.5 keV line from clusters of galaxies
 - XMM-Newton (and Chandra) results
 - Suzaku results
 - ASTRO-H SXS results
 - Emission from the Milky-way halo by Suzaku
- Axion and ALP search using the earth's magnetic field
- Monochromatic solar-axion search
 - TES microcalorimeter development and ground applications
 - Signal multiplexing (MUX) for large format TES
 - TES microcalorimeter for solar-axion search

Sterile neutrinos

- Right-handed neutrinos
 - Neutrino oscillation
- N_1 (\sim keV) can be a dark matter candidate
 - Production scenarios exist
 - Warm dark matter
 - may solve sub-halo and core-cusp problems
- Radiative decay modes exist in addition to dominant decay mode

$$N_1 \rightarrow \nu + \gamma$$

(e.g. Boyarsky 2009)

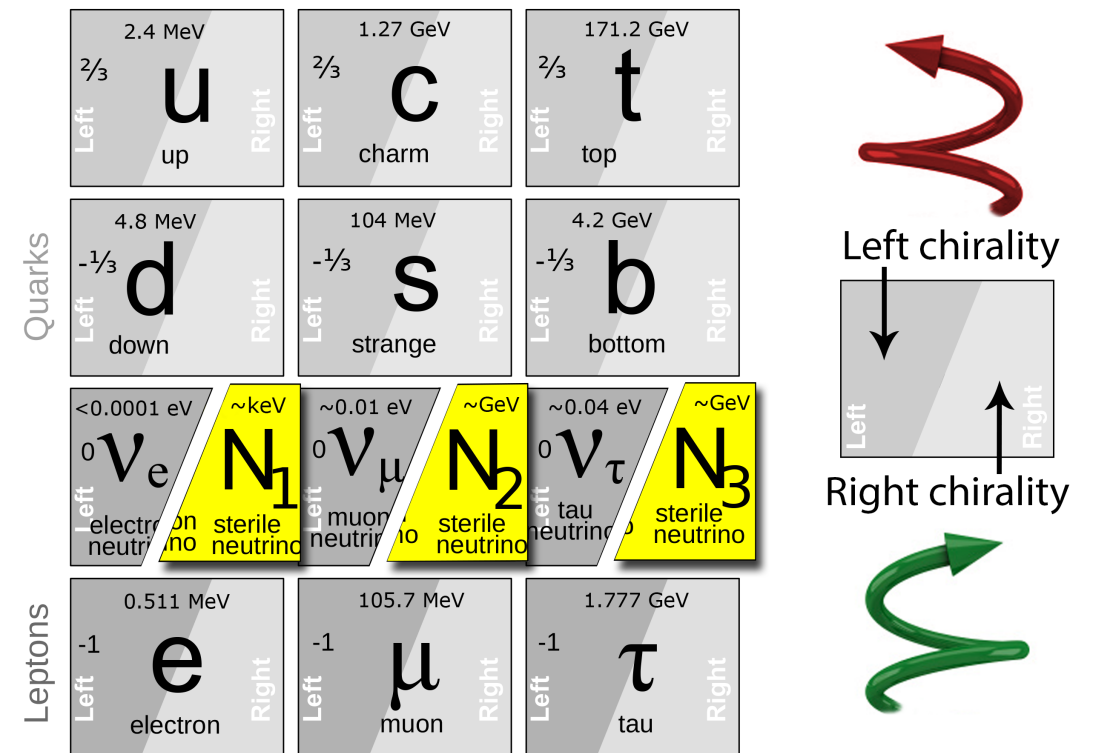


Astronomical search

Monochromatic emission

$$E = m_{N_1}/2$$

(Abazajian+ 2001)



<http://wwwhome.lorentz.leidenuniv.nl/~boyarsky/>

Where to observe?

- Clusters of galaxies
- Dwarf and/or spiral galaxies
- Milky-way halo

All observations so far are background limited (and not photon limited).

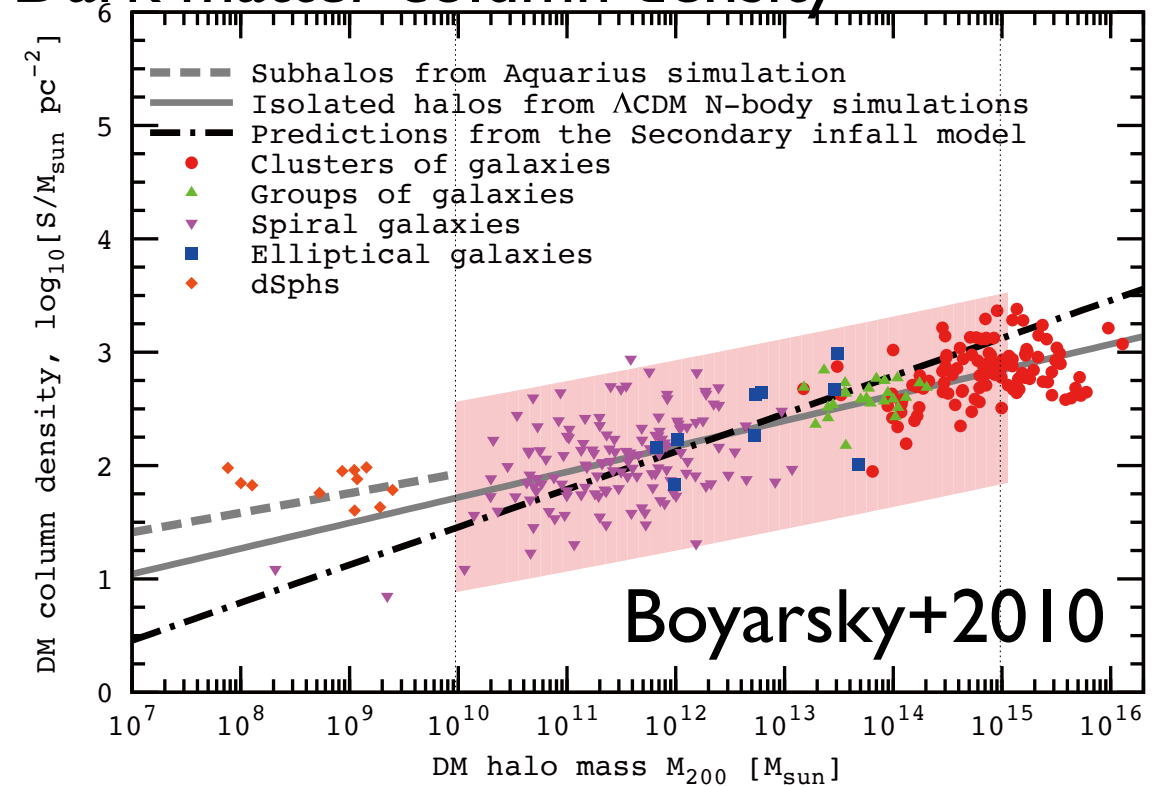
$$\text{Figure of merit} = \frac{\text{DM column density}}{\sqrt{\text{Baryon surface brightness}}}$$

	Milky-way halo	Dwarfs	Spirals	Clusters
Figure of merit	29	20	13	4

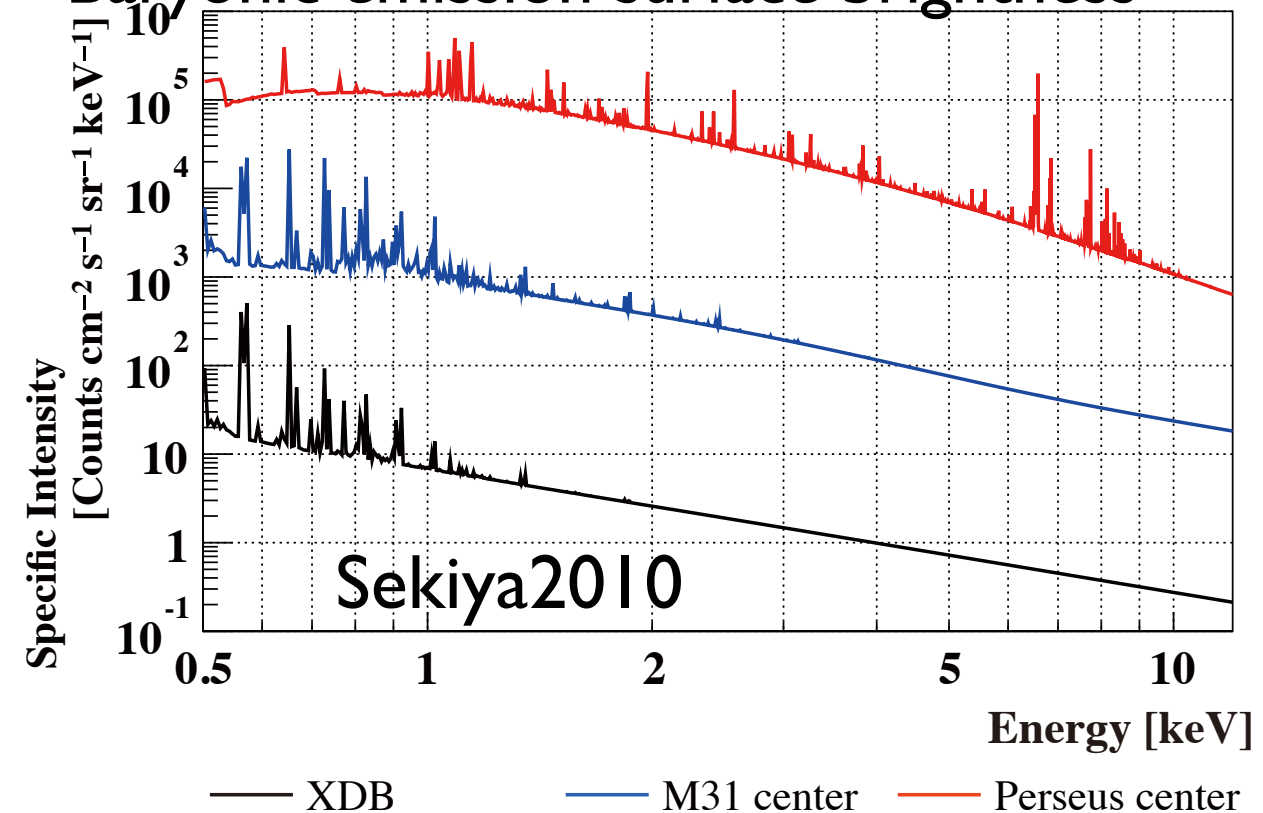
Assuming that the object is extended all over the field of view

$$\text{Unit is } \frac{M_{\odot} \text{ pc}^{-2}}{\sqrt{\text{photons cm}^{-2} \text{ s}^{-1} \text{ sr}^{-1} \text{ keV}^{-1} @ 2\text{keV}}}$$

Dark matter column density



Baryonic emission surface brightness



Instruments to use

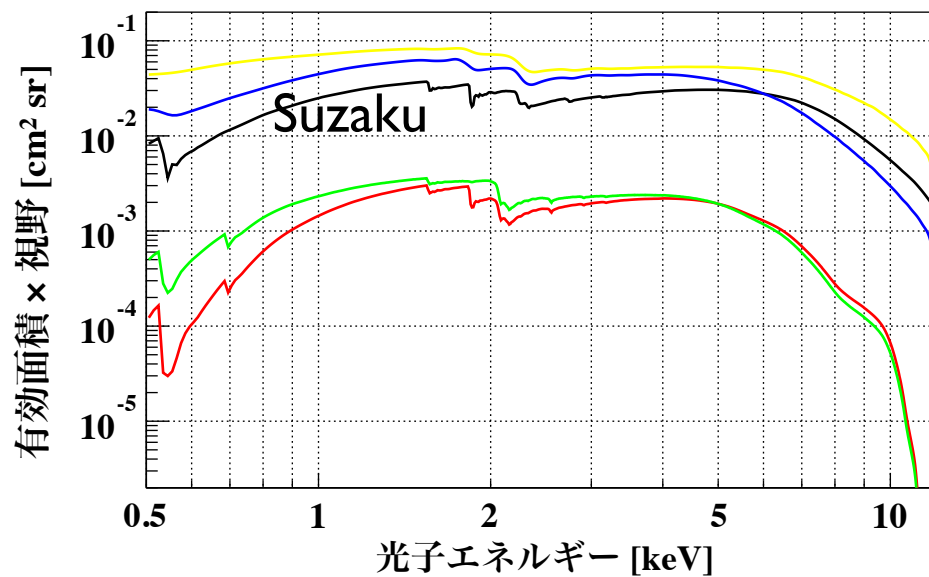
「Chandra/ACIS」 「XMM-Newton/PN, MOS」 「すざく/XIS」 の性能比較

Suzaku observation of Milky-way halo is the best combination.



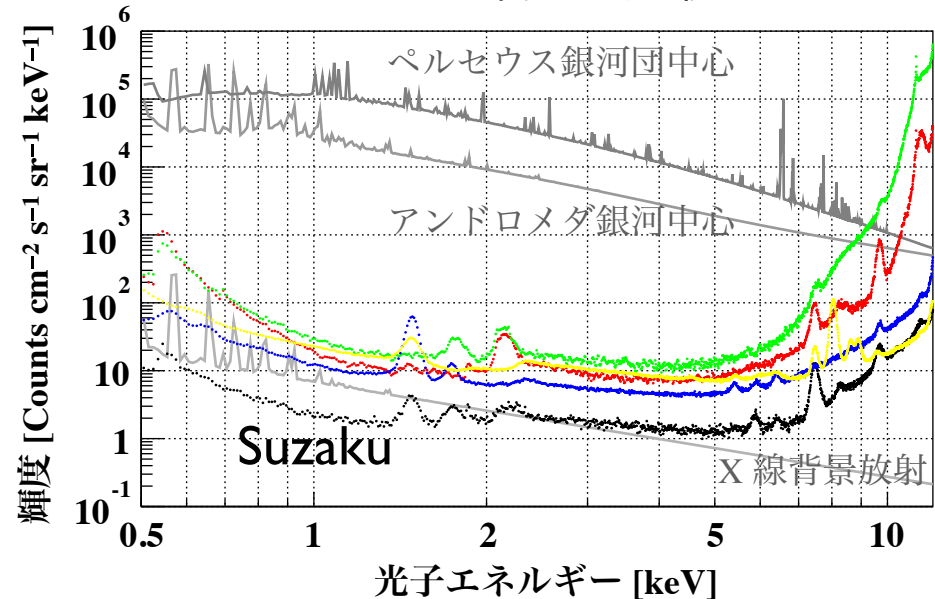
	Chandra/ACIS	XMM-Newton/MOS+PN	Suzaku/XIS
視野 [amin ²]	8.3 × 8.3 × (4FI + 6BI)	~700 × (2MOS + 1PN)	17.8 × 17.8 × (3FI + 1BI)
エネルギーバンド [keV]	0.3 – 12	0.15 – 15	0.2 – 12
エネルギー分解能 [eV]	50 – 200	50 – 200	50 – 200
有効面積 @ 1 keV [cm ²]	200 (4FI), 400 (6BI)	800 (2MOS), 1200 (PN)	660 (3FI), 320 (BI)
NXB 輝度 [cm ⁻² s ⁻¹ sr ⁻² keV ⁻¹]	10 – 1000 (不安定)	5 – 100 (不安定)	1 – 10 (安定)

有効面積 × 視野の比較



Suzaku/4XIS Chandra/ACIS-I XMM-Newton/2MOS
Chandra/ACIS-S XMM-Newton/PN

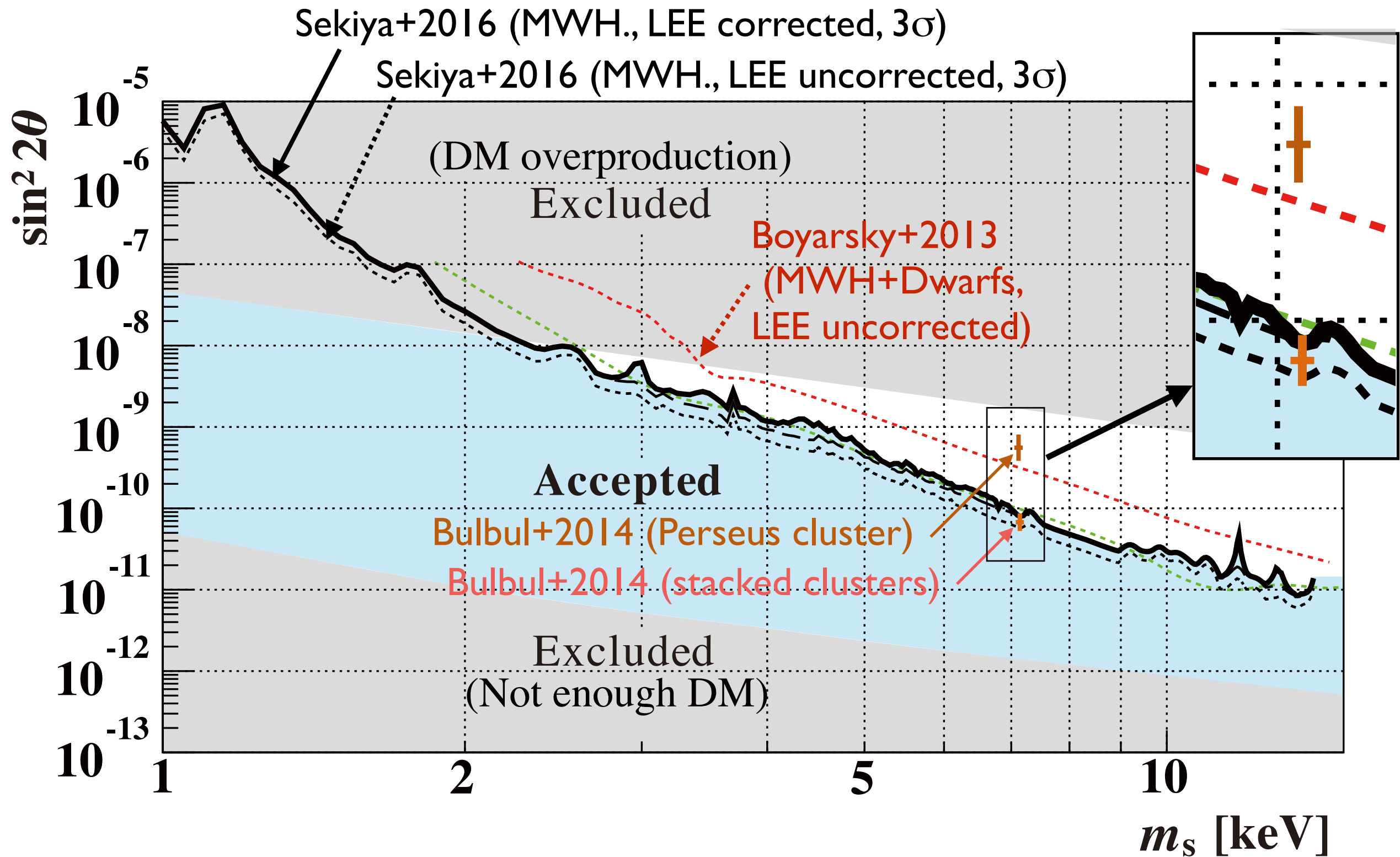
NXB 輝度の比較



Suzaku/4XIS Chandra/ACIS-I XMM-Newton/2MOS
Chandra/ACIS-S XMM-Newton/PN

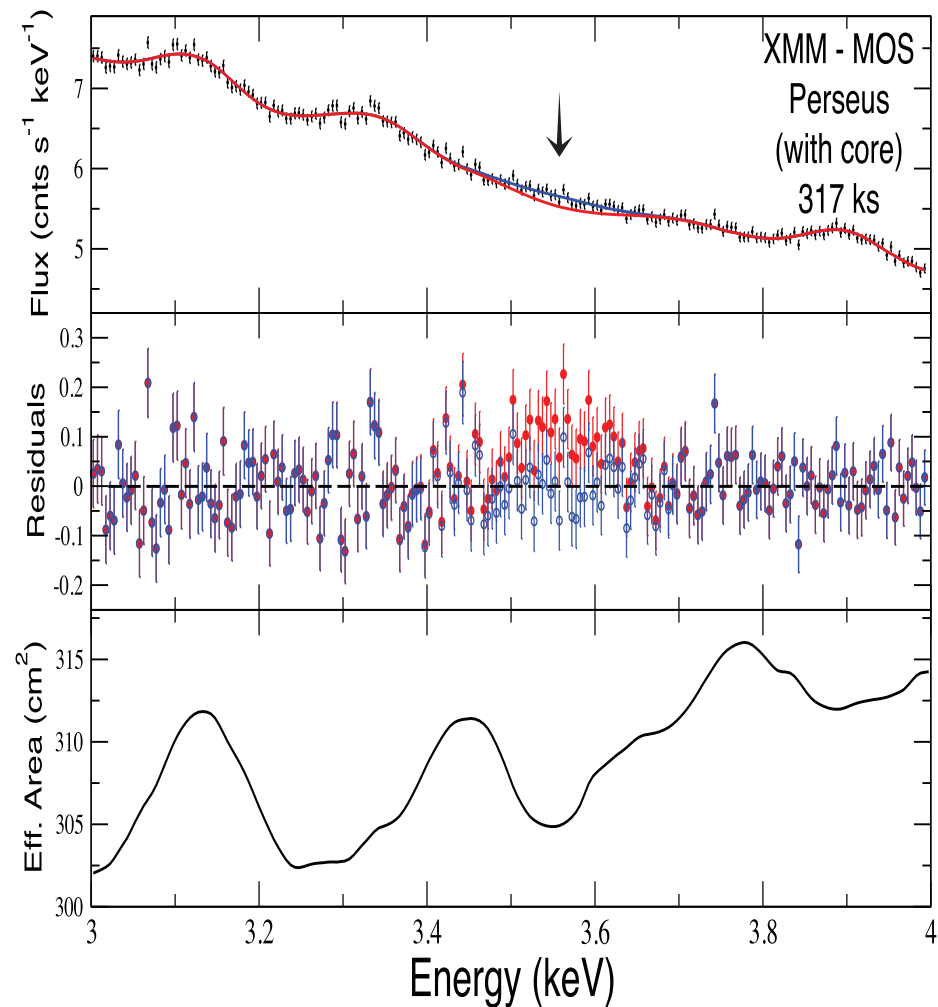
From Yamasaki+ 2017

Present astronomical constraints on sterile neutrinos

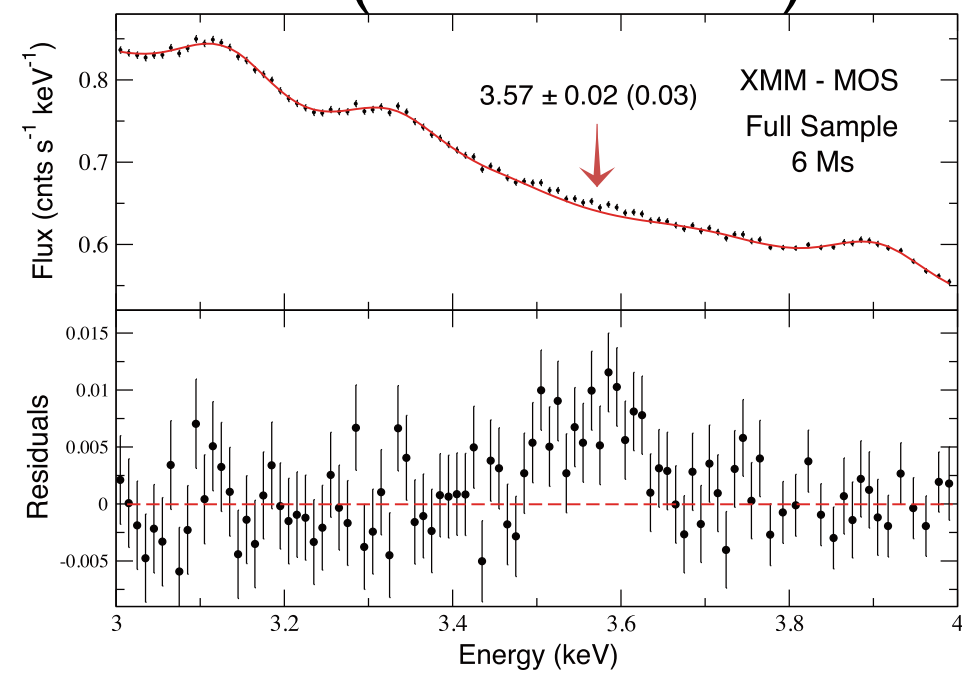


Cluster 3.5 keV line (Bulbul+2014)

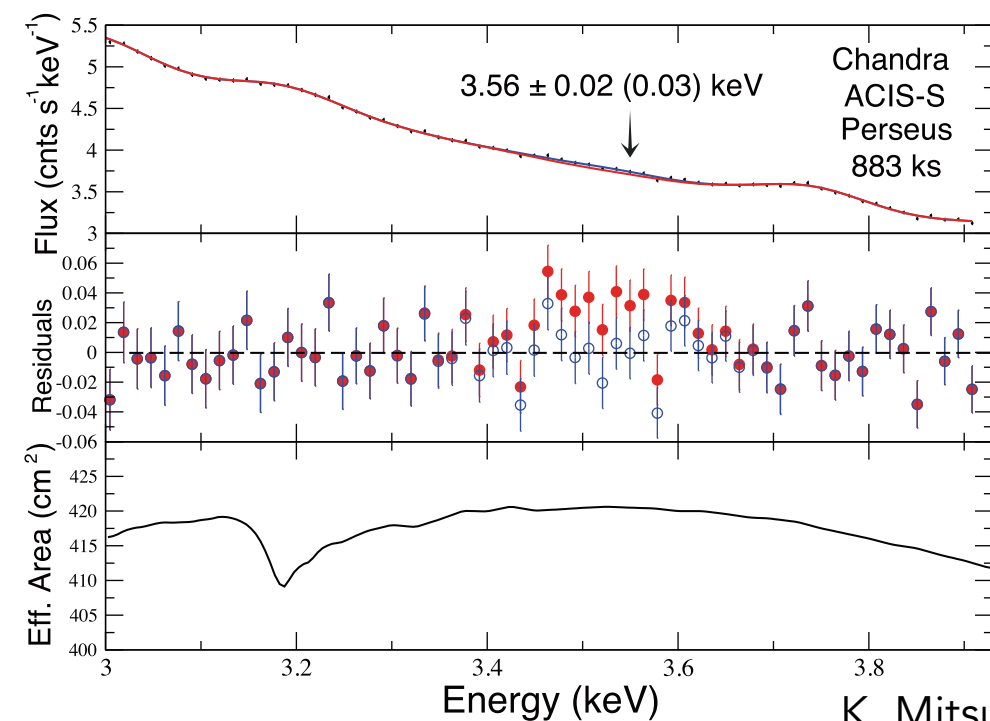
Perseus cluster (XMM-Newton MOS)



78 clusters stacked after z correction (XMM-Newton)



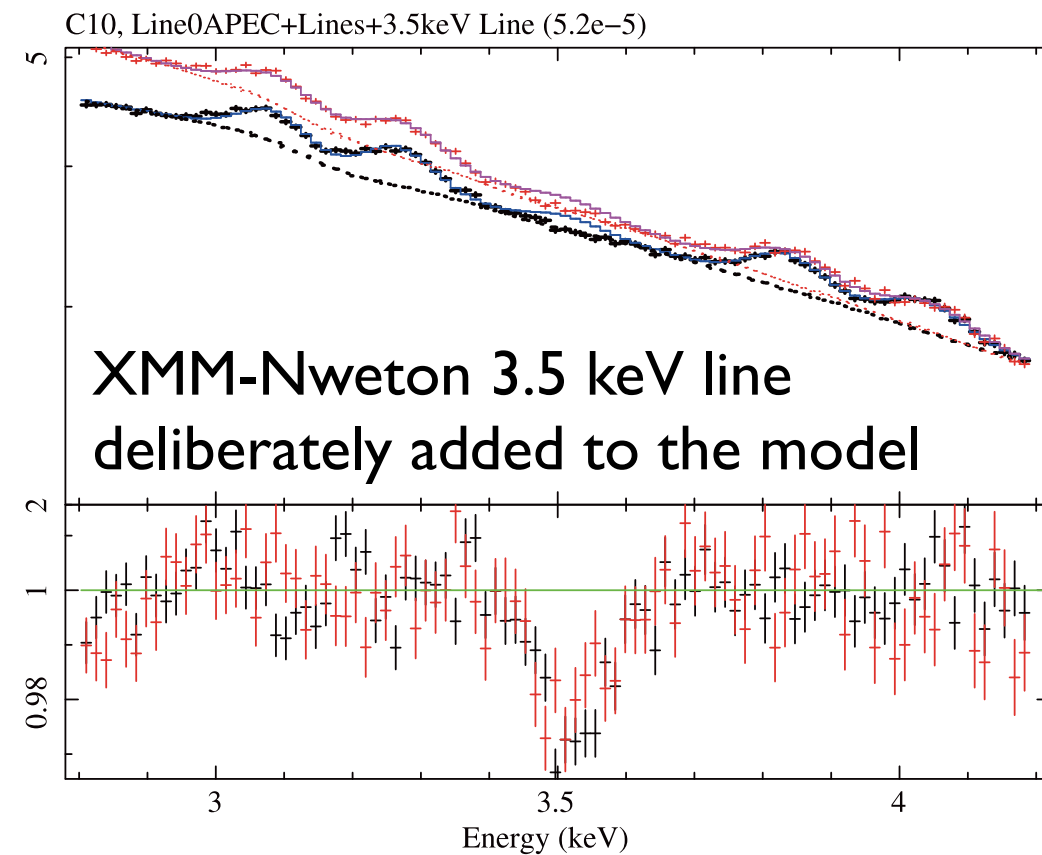
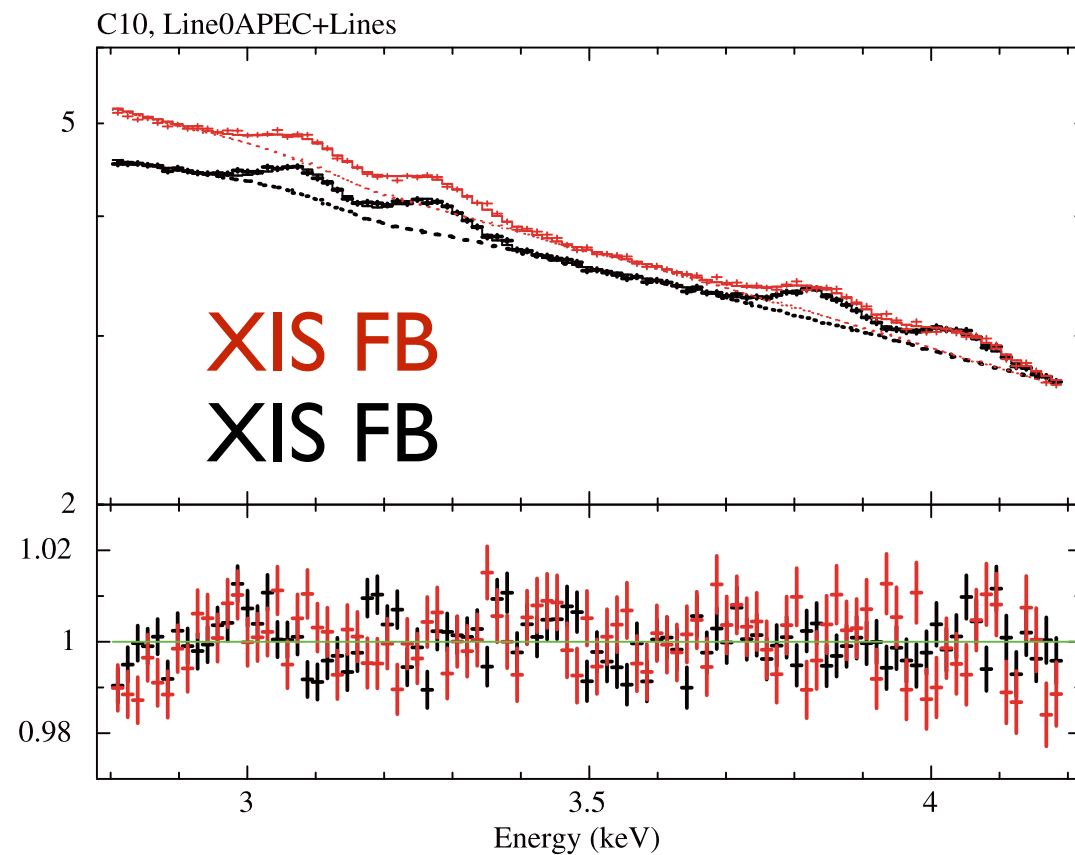
Perseus cluster (Chandra ACIS-S)



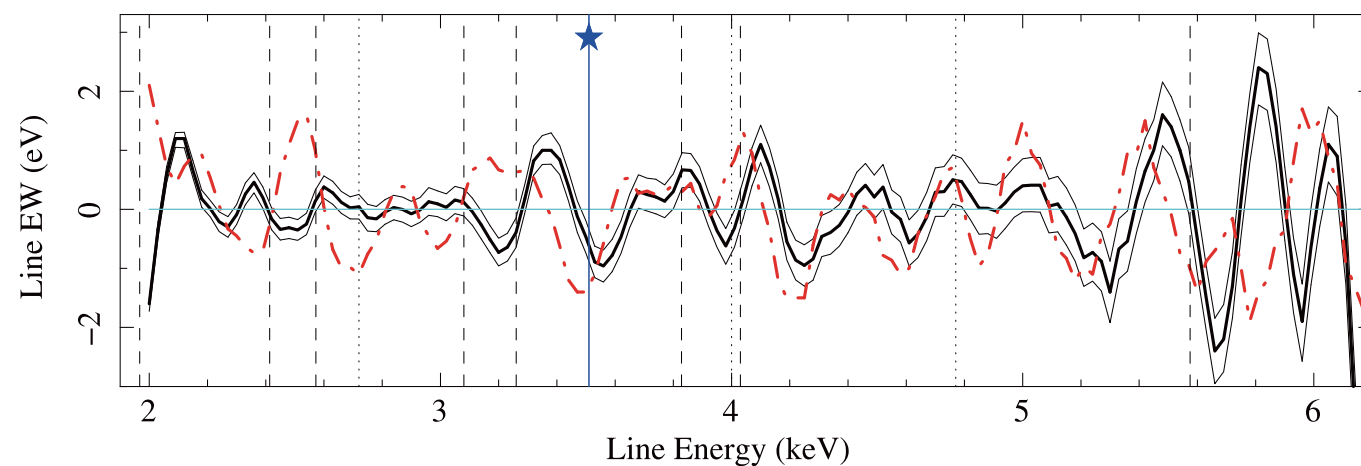
Caveats and issues of 3.5 keV line

- Caveats discussed in Bulbul+ 2014:
 - The equivalent width of the line is only ~ 1 eV, while the energy resolution is ~ 100 eV. Thus the excess is only $\sim 1\%$ of continuum spectrum. Uncertainties in continuum model significantly affects the results.
- Issues found in their results
 - Two different sets of sensors, MOS and PN, of XMM-Newton gives inconsistent intensities of the Perseus cluster residual emission.
 - Centroid energies of MOS and PN for stacked spectra are inconsistent within the statistical errors.
 - Residual intensity of Perseus cluster is ~ 10 times larger than that of the stacked spectrum.

Suzaku Perseus results (Tamura+2015)

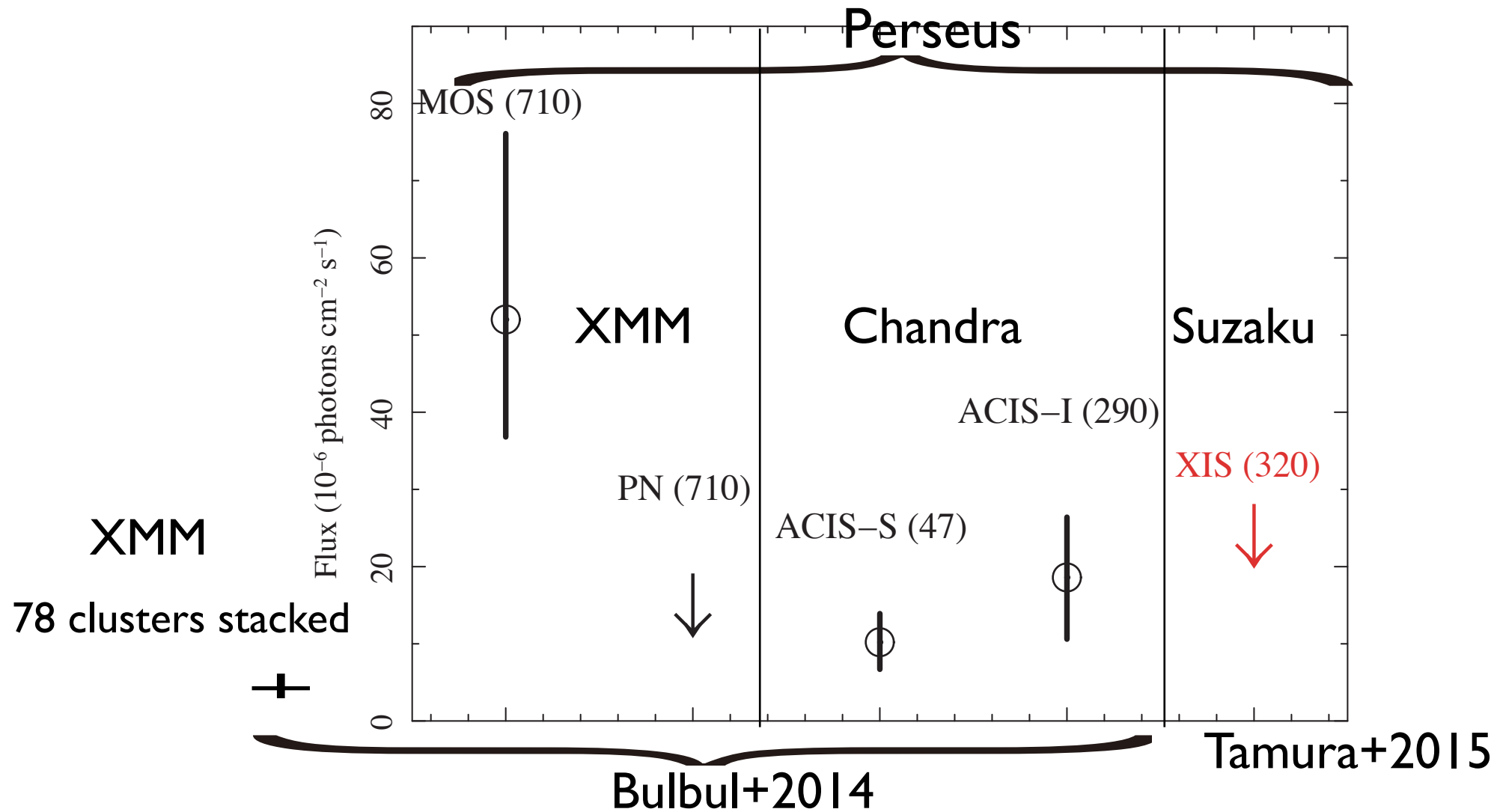


“Line search”



$1-\sigma$ sensitivity is ~ 1 eV EW level.

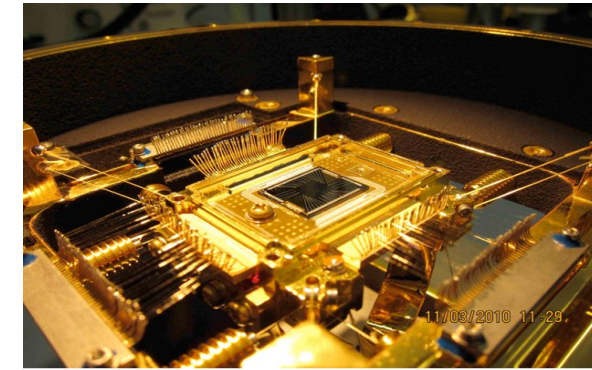
Perseus results compared



Detector	Area (cm^2)	FOV (arcmin^2)	exp (ks)	Area \times exp ($\text{}$)	Area \times exp \times FOV ($\text{}$)
MOS	300	710	317	95.1K	67.5M
PN	700	710	38	26.6K	18.9M
XIS/FI	260	320	1040	270K	86.5M
XIS/BI	260	320	530	138K	44.1M
total	-	-	-	408K	131M

ASTRO-H SXS Perseus

- Improves energy resolution by a factor of 20.
- Energy resolution (5eV) becomes the same order of the equivalent widths (~ 1 eV), which makes uncertainty of continuum much less important.
- Major drawbacks are smaller effective area and field of view; sensitivity is limited by photon statistics



X-ray microcalorimeter
operating at 50mK
Kelley+2017

Suzaku XIS

ASTRO-H SXS

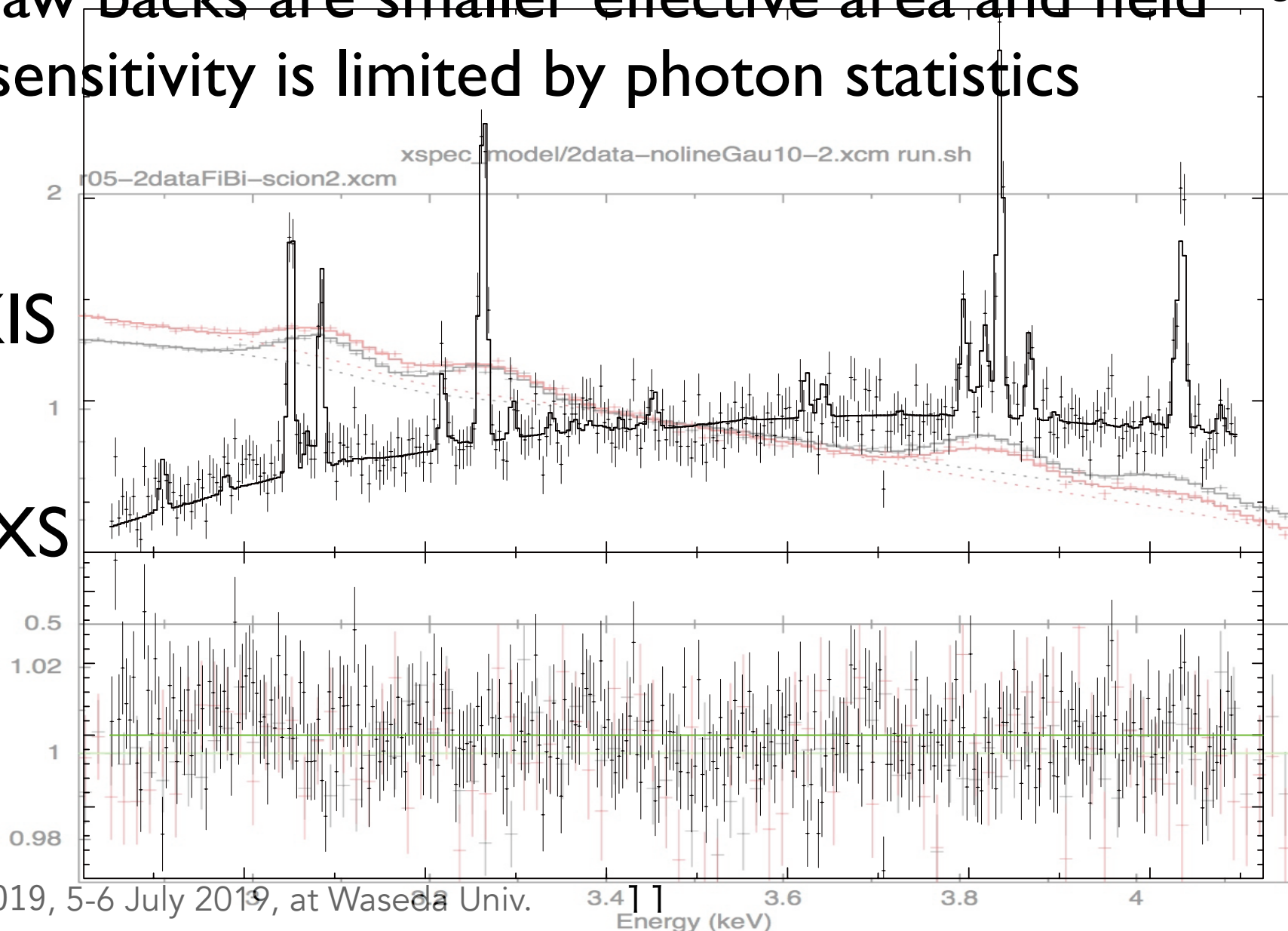


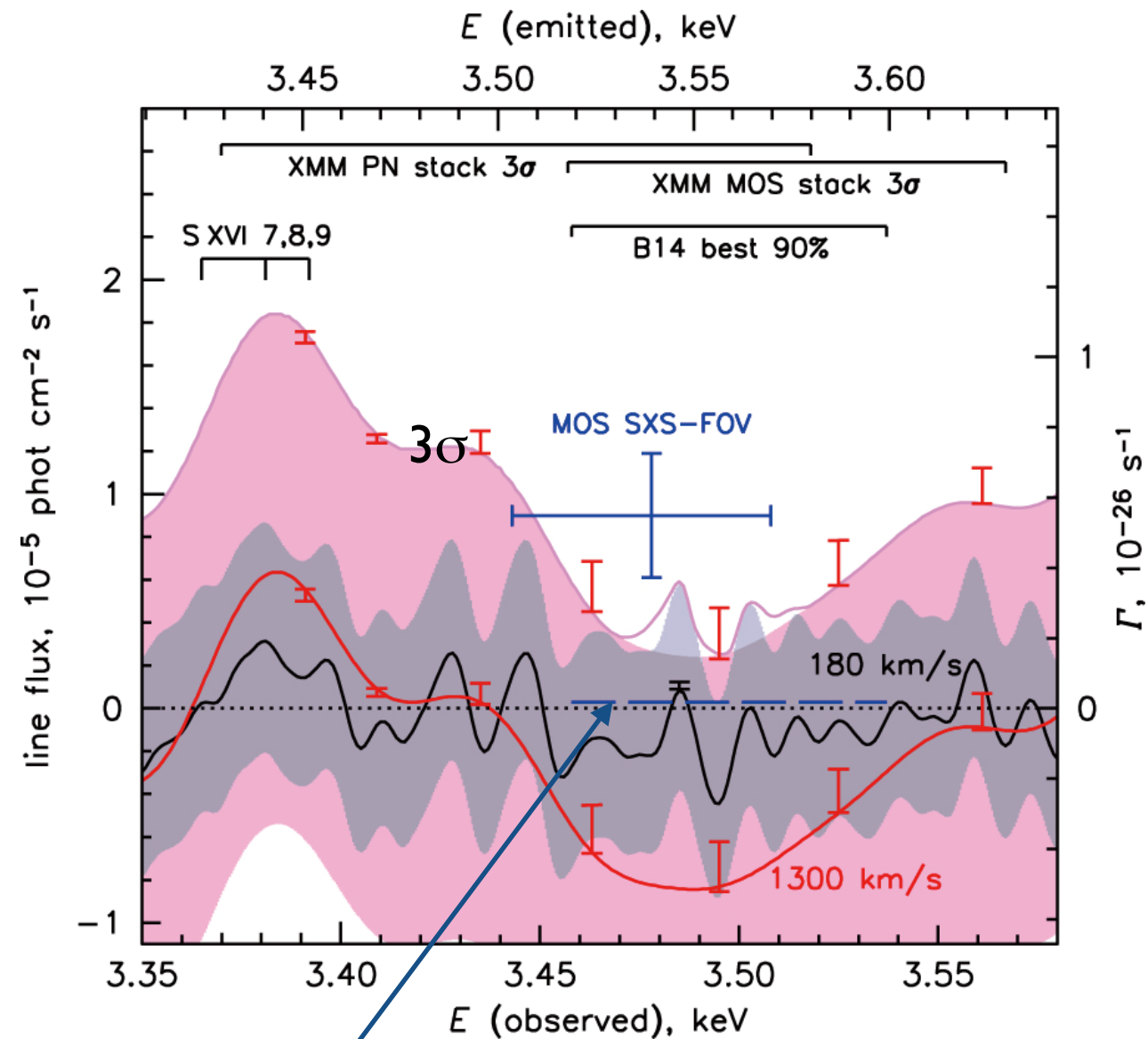
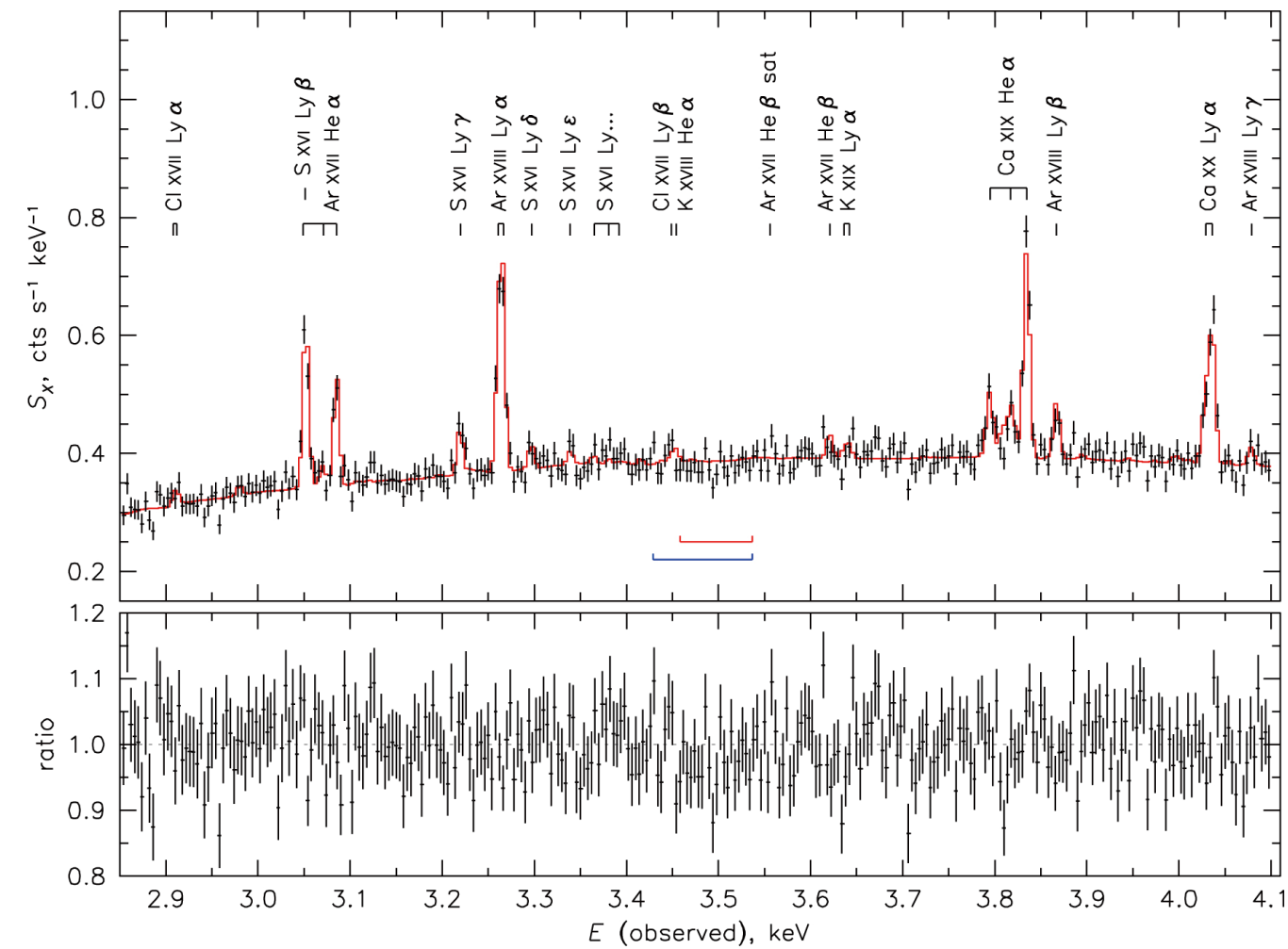
Figure from
Tamura 2017

K. Mitsuda, ISAS, JAXA

ASTRO-H SXS Perseus

Hitomi collaboration 2017

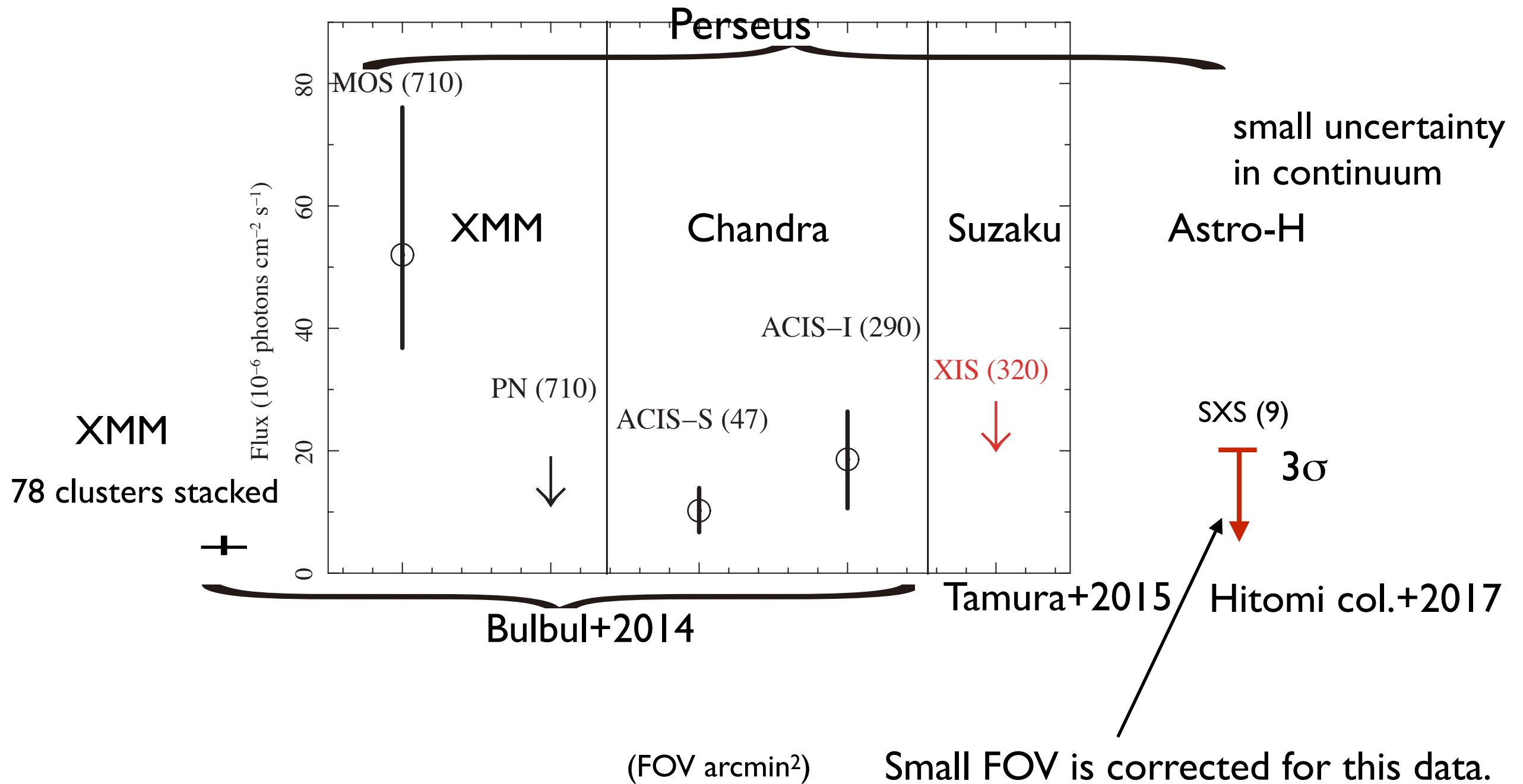
XMM-Newton MOS Perseus intensity was excluded at a 3σ confidence limit.
 However, intensity of stacked clusters is not excluded.



180 km/s: thermal velocity of a proton
 1300 km/s: velocity dispersion of galaxies

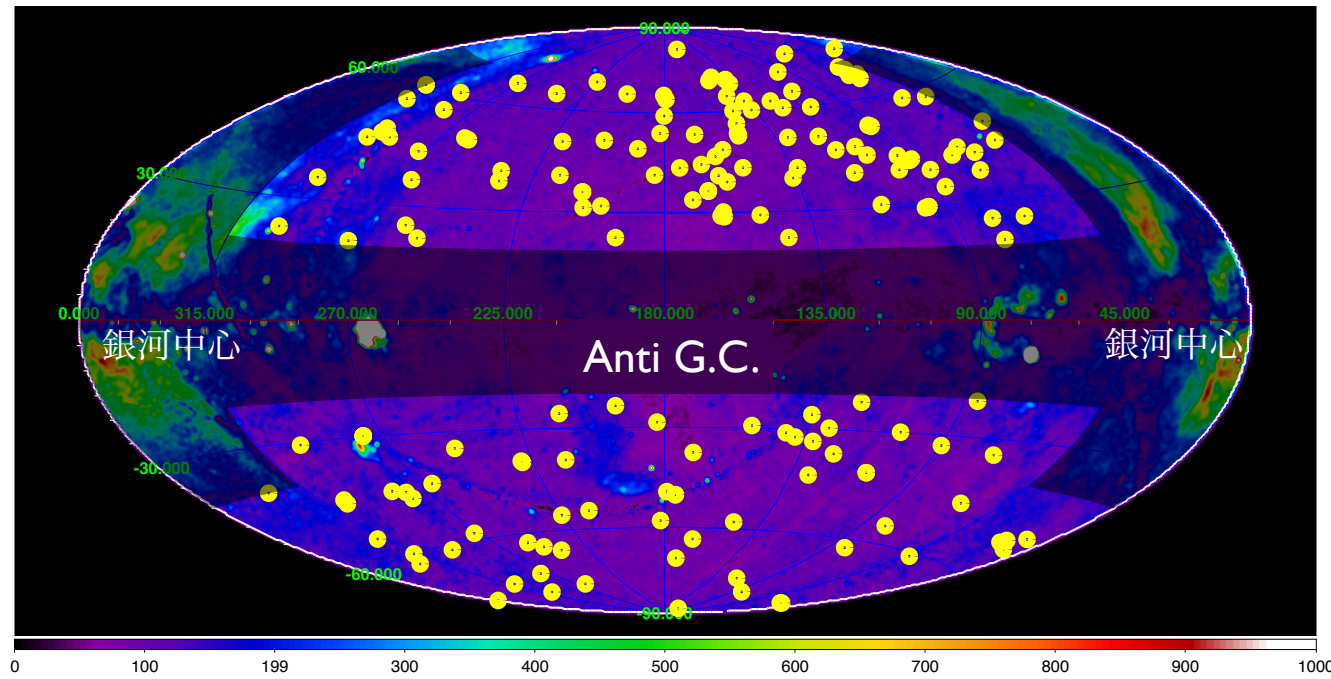
Intensity of XMM stacked clusters

Perseus results compared

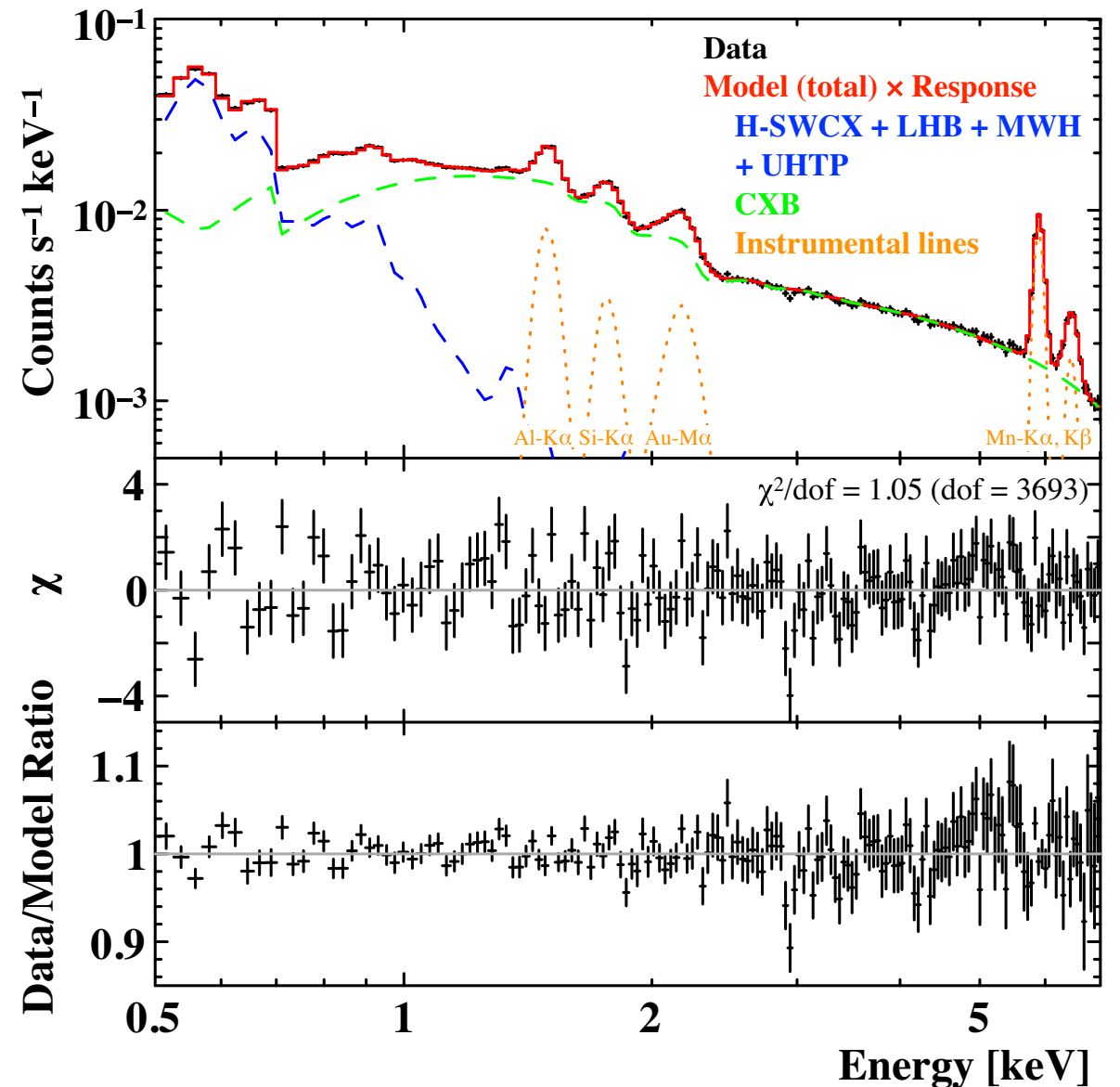


Milky-way halo: Suzaku results

Sekiya+2016



- 187 fields with faint sources removed.
- 31 Ms integration time
~ 20 % of total Suzaku observation time.



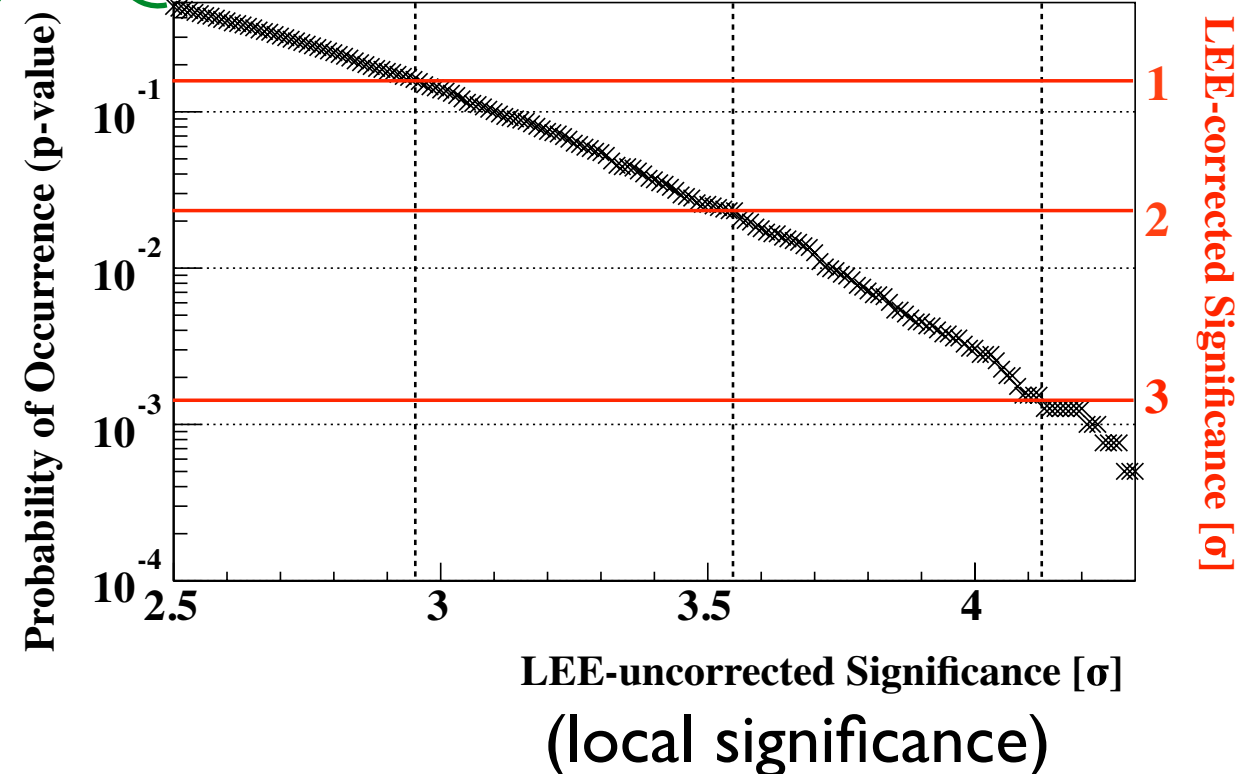
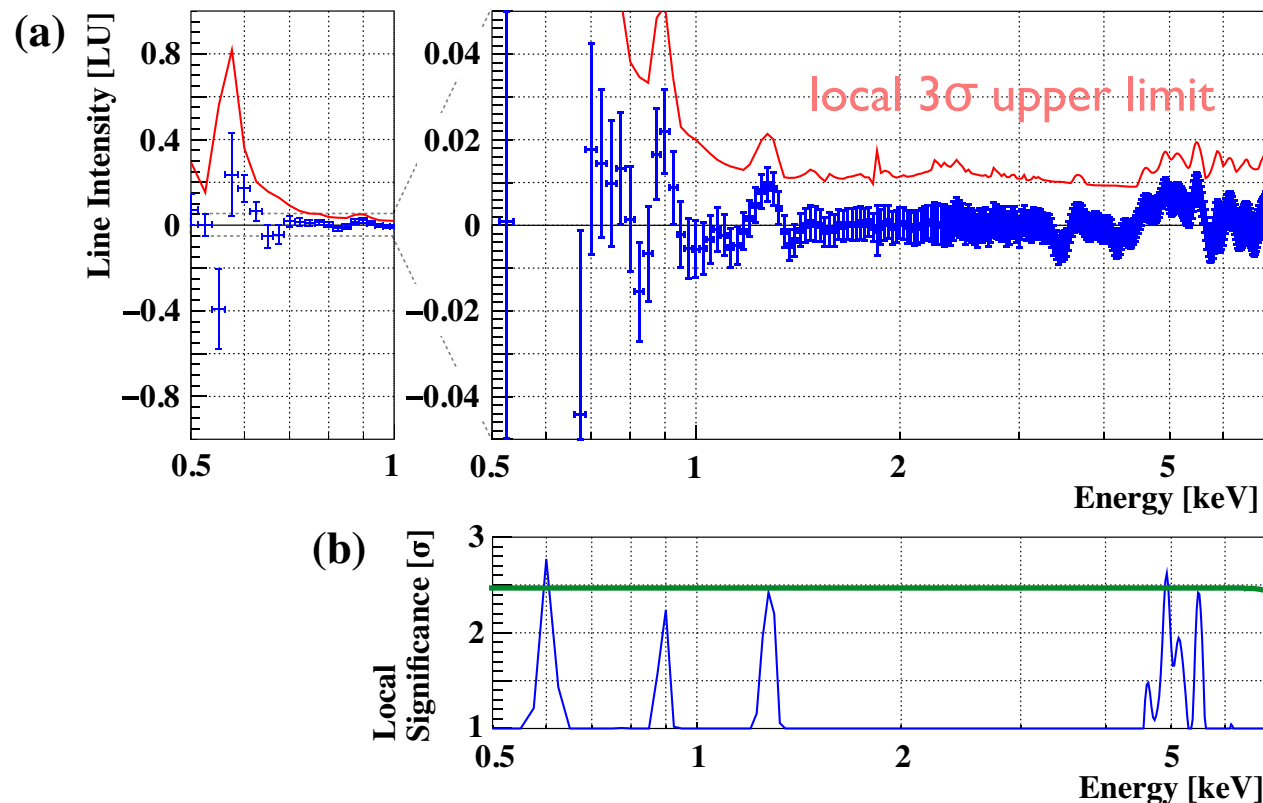
Spectrum is modeled well with

- Non X-ray background
- Heliosphere + Local Bubble
- Hot ISM in Milky-way halo
- Faint extragalactic sources

Line search and Look elsewhere effect (LEE)

Line search

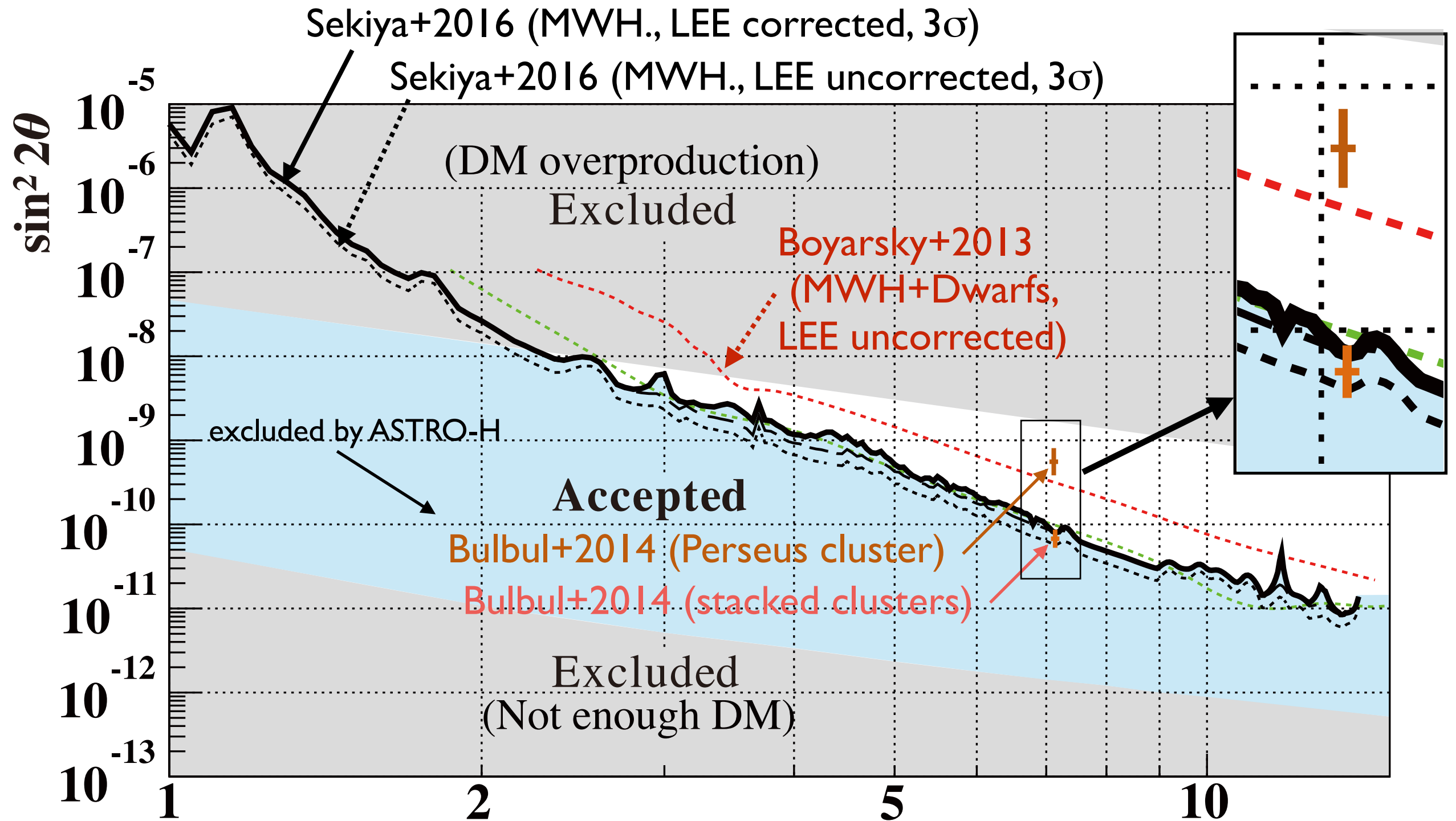
Number of independent searches across the spectrum determines the final upper limit, which is determined with Monte-Carlo simulations



Lines with $\geq 2.5\sigma$ local significance are expected to appear with $\sim 40\%$ probability at some energies in the spectrum. This is consistent with the observational results.

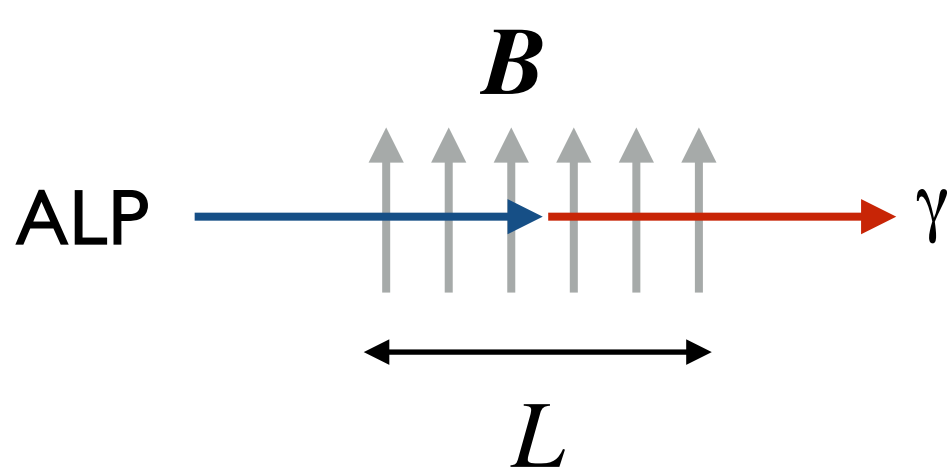
Comparison of Suzaku MW result with 3.5 keV line

Intensity of stacked clusters Bulbul+2014 is statistically excluded at a 3σ confidence. However, because of uncertainty in column density, we cannot perfectly ruled it out.



Axion and ALP search using the earth magnetic field

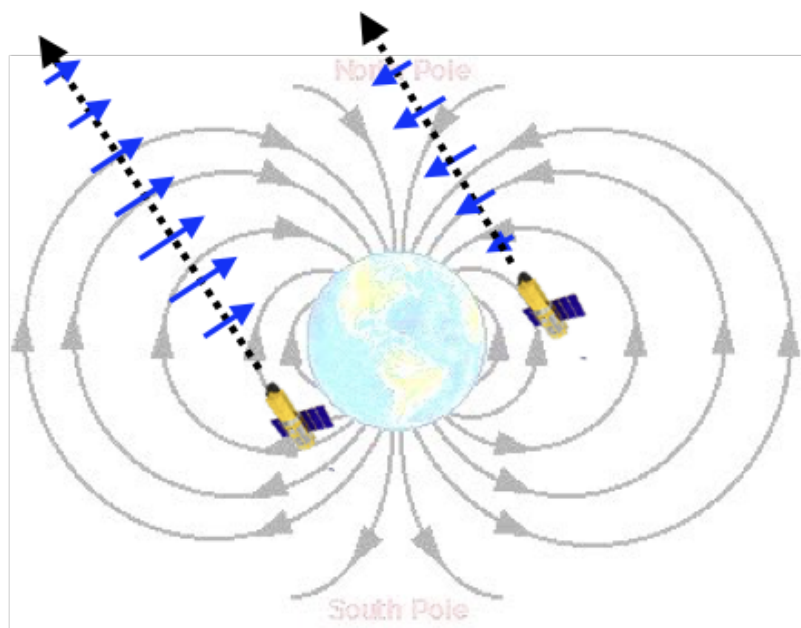
The inverse Primakoff effect



$$P_{a \rightarrow \gamma} \sim 2 \times 10^{-21} \left(\frac{g_{a\gamma\gamma}}{10^{-10} \text{ GeV}^{-1}} \right)^2 \left(\frac{B_{\perp} L}{\text{T m}} \right)^2$$

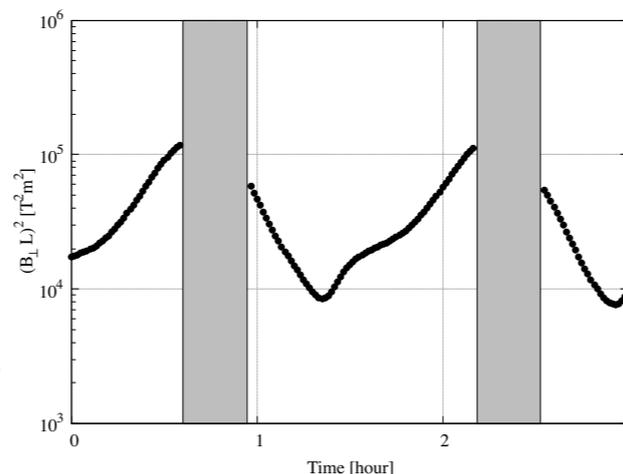
$$\text{for } m_a < 10^{-6} \text{ eV} \left(\frac{E_a}{1 \text{ keV}} \right)^{\frac{1}{2}} \left(\frac{L}{10^4 \text{ km}} \right)^{-\frac{1}{2}}$$

Low-earth orbits or line sight through the earth



← Blue arrow: Magnitude of B_{\perp}
 ← Dotted arrow: Line-of-sight

$$B^2 L^2 = 10^5 \text{ to } 10^6 \text{ m}^2 \text{T}^2 \gg B^2 L^2 = 6.4 \times 10^3 \text{ m}^2 \text{T}^2$$

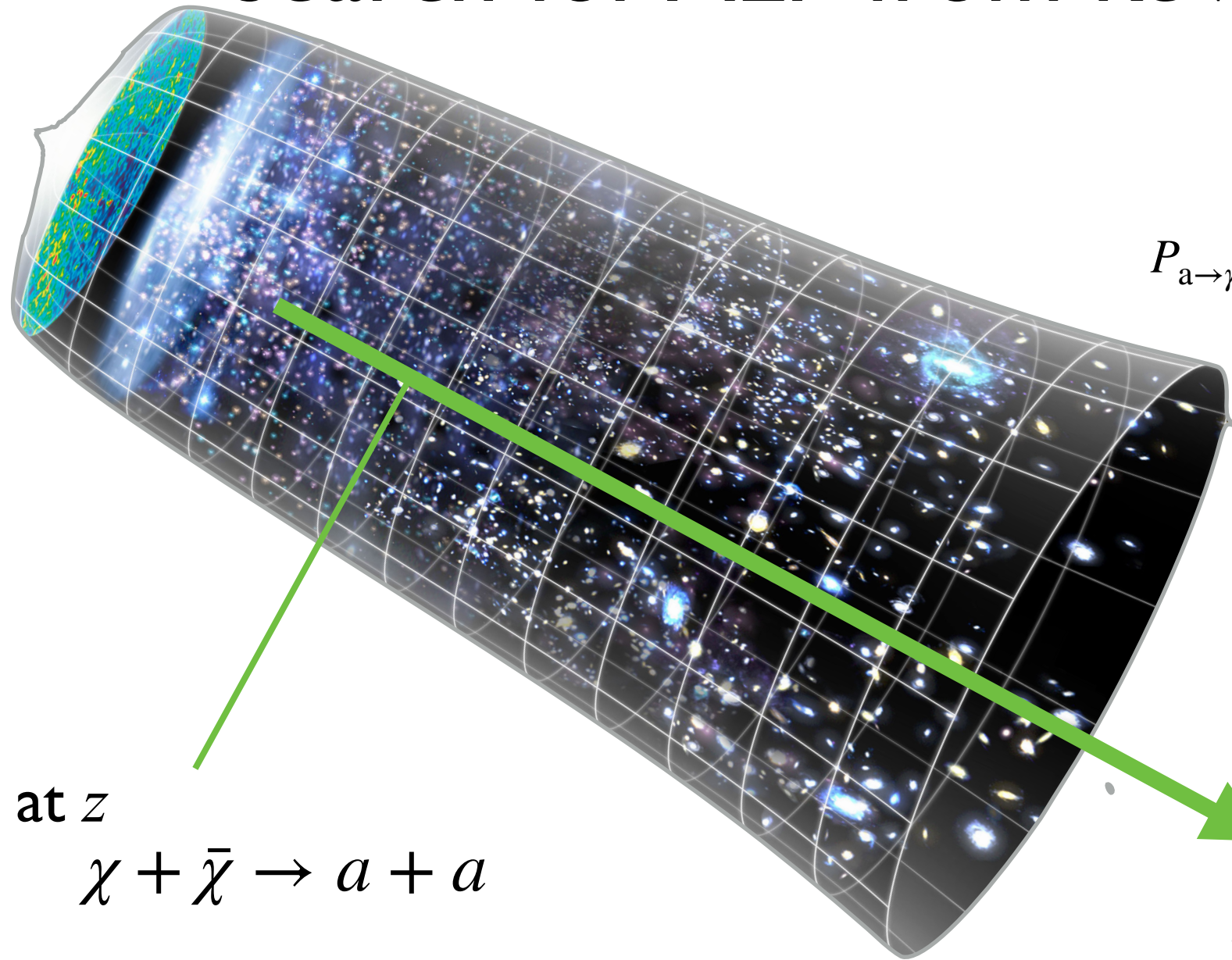


Ground experiments
 superconductor magnet + cavity

CAST

Large BL
 Sensitive mass range limited by large L

Search for ALP from keV dark matter



at z
 $\chi + \bar{\chi} \rightarrow a + a$

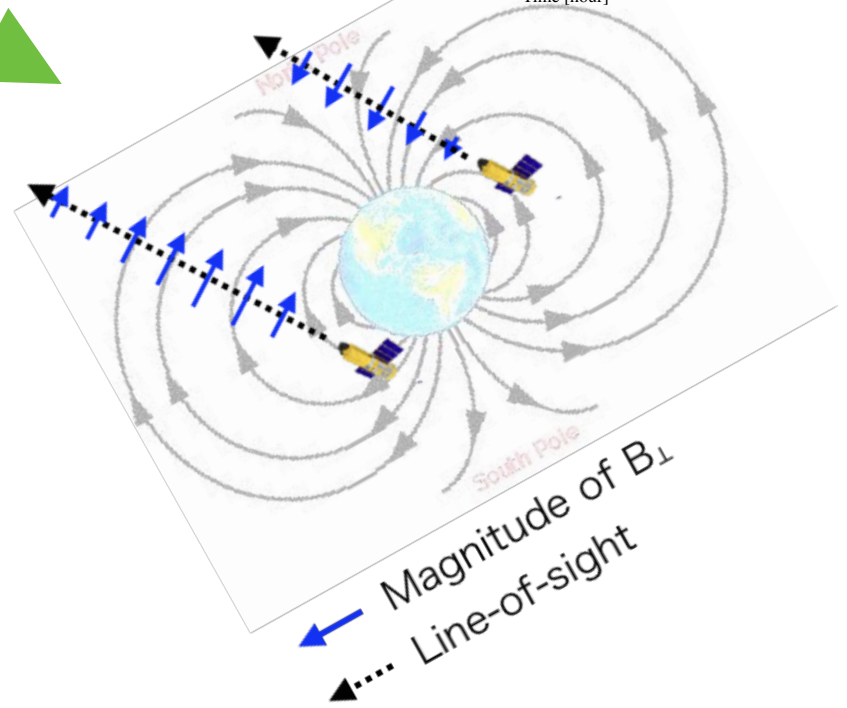
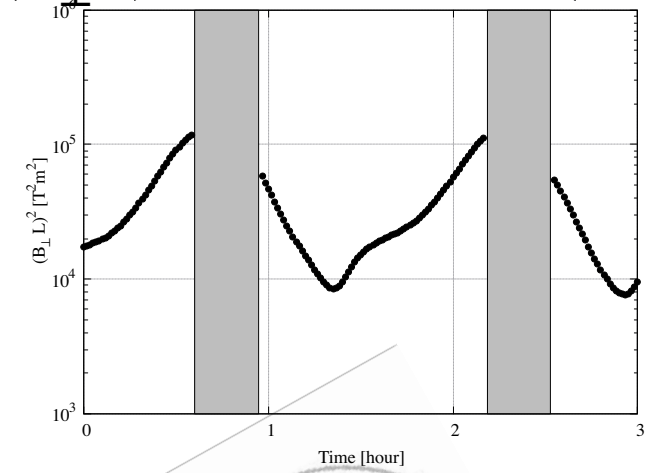
Integrating over z , ALP spectrum will be

$$\frac{dN}{dE} \propto E^{+0.5} \quad (\text{e.g. Asaka+1998})$$

The inverse Primakoff effect

$$P_{a \rightarrow \gamma} \sim 2 \times 10^{-21} \left(\frac{g_{a\gamma\gamma}}{10^{-10} \text{ GeV}^{-1}} \right)^2 \left(\frac{B_{\perp} L}{\text{T m}} \right)^2$$

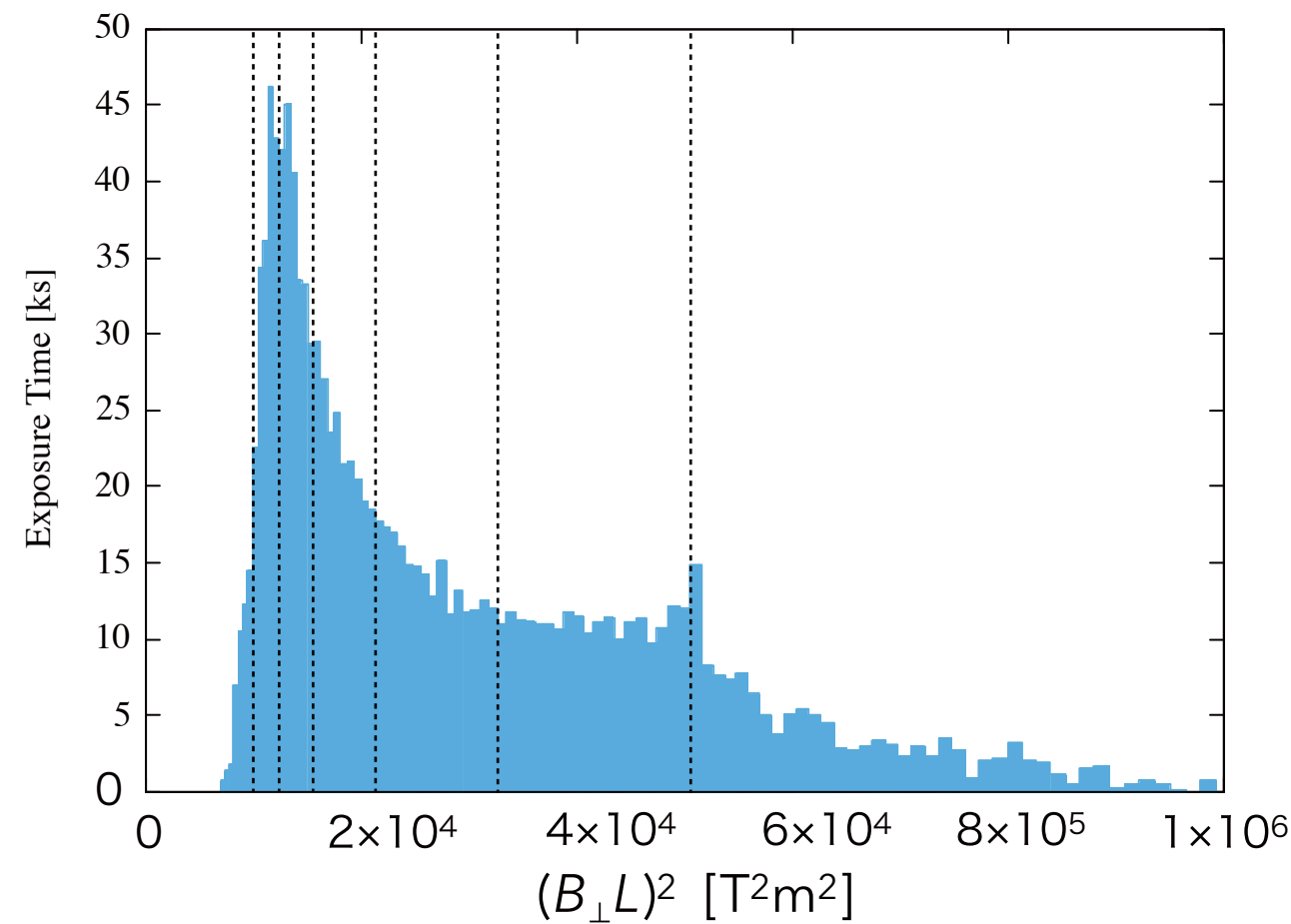
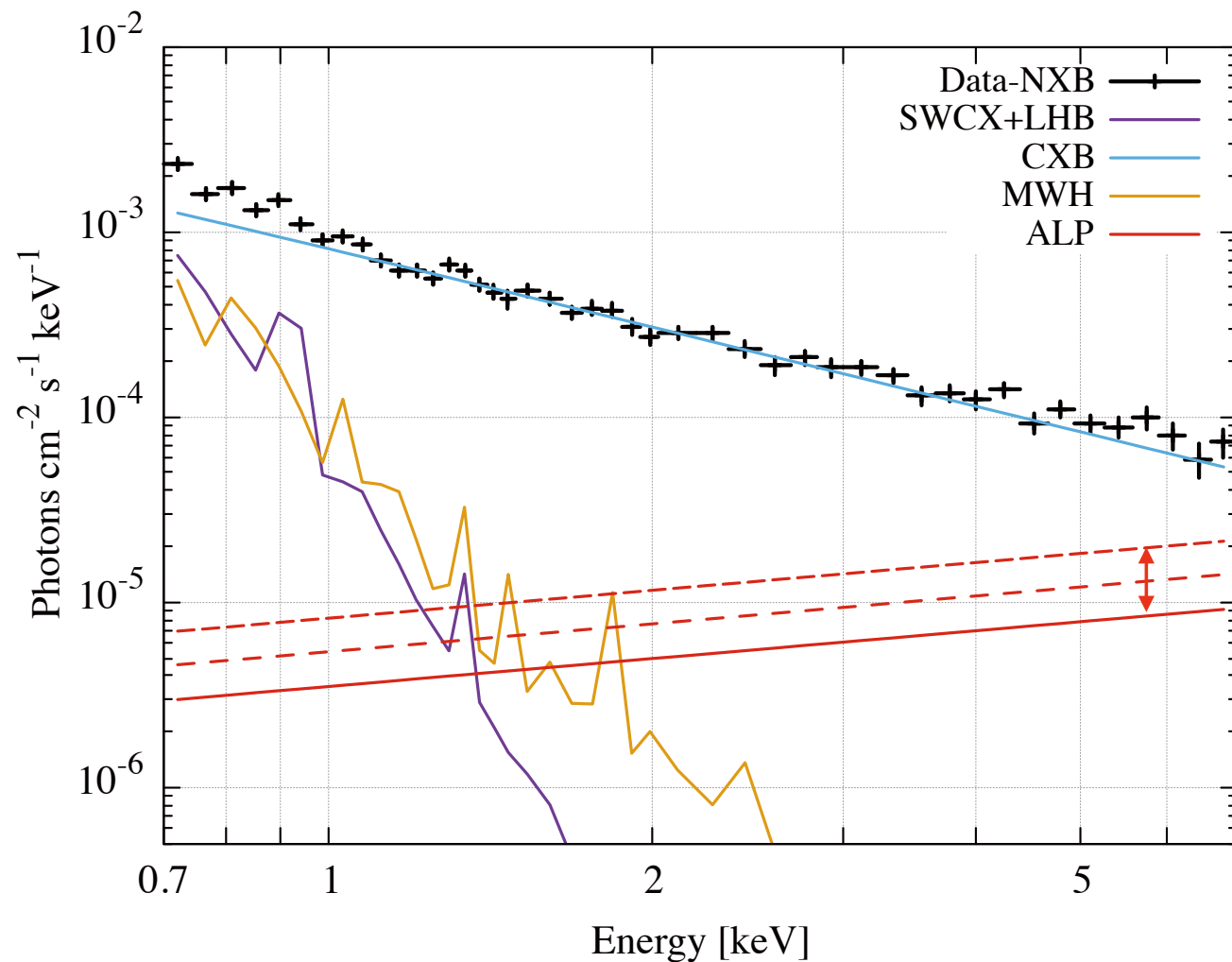
$$(B_{\perp} L)^2 = 10^4 - 10^5 (\text{T m})^2$$



Search for ALP

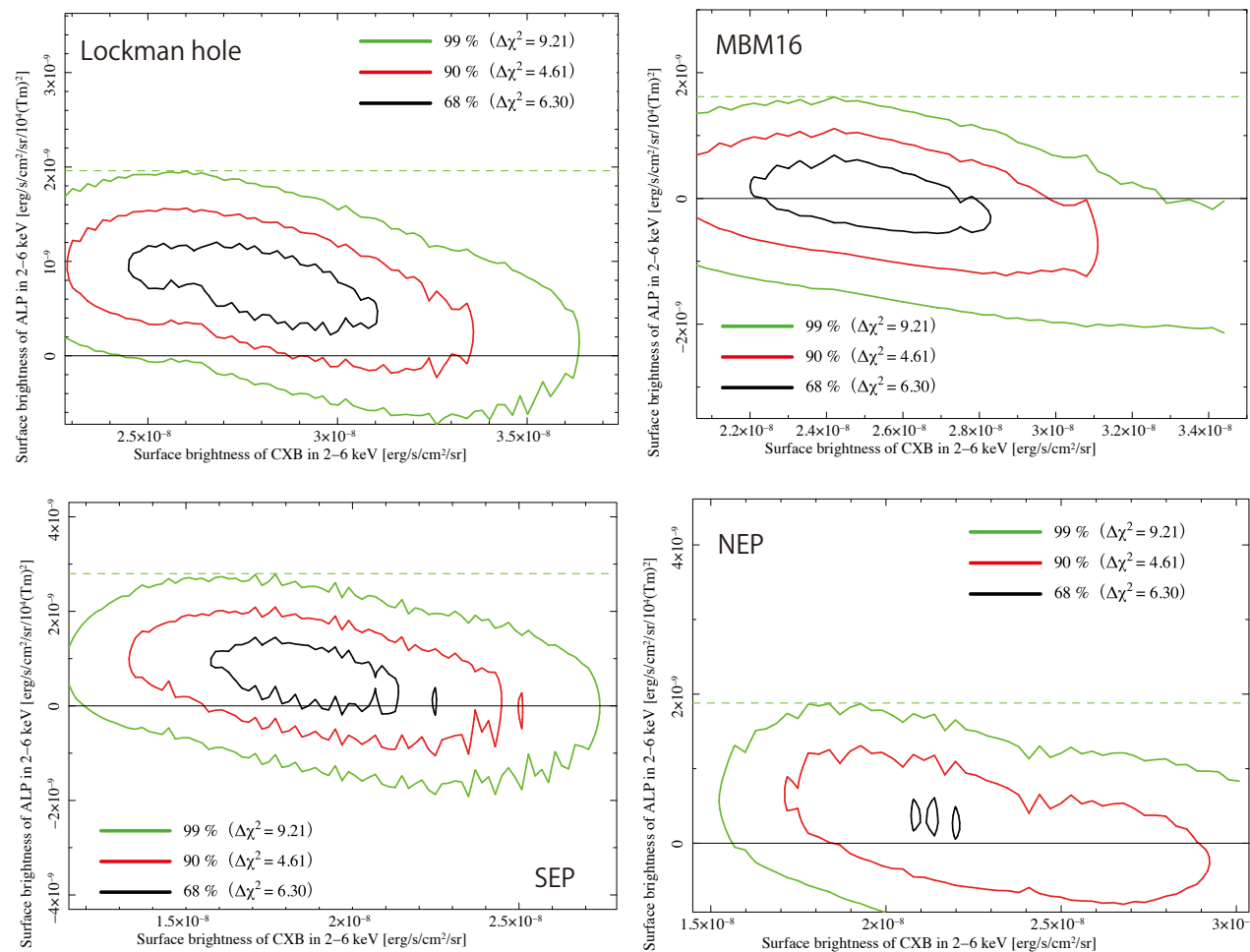
Yamamoto+2019

Search for a spectral component which is $\propto (B_{\perp}L)^2 E^{0.5}$

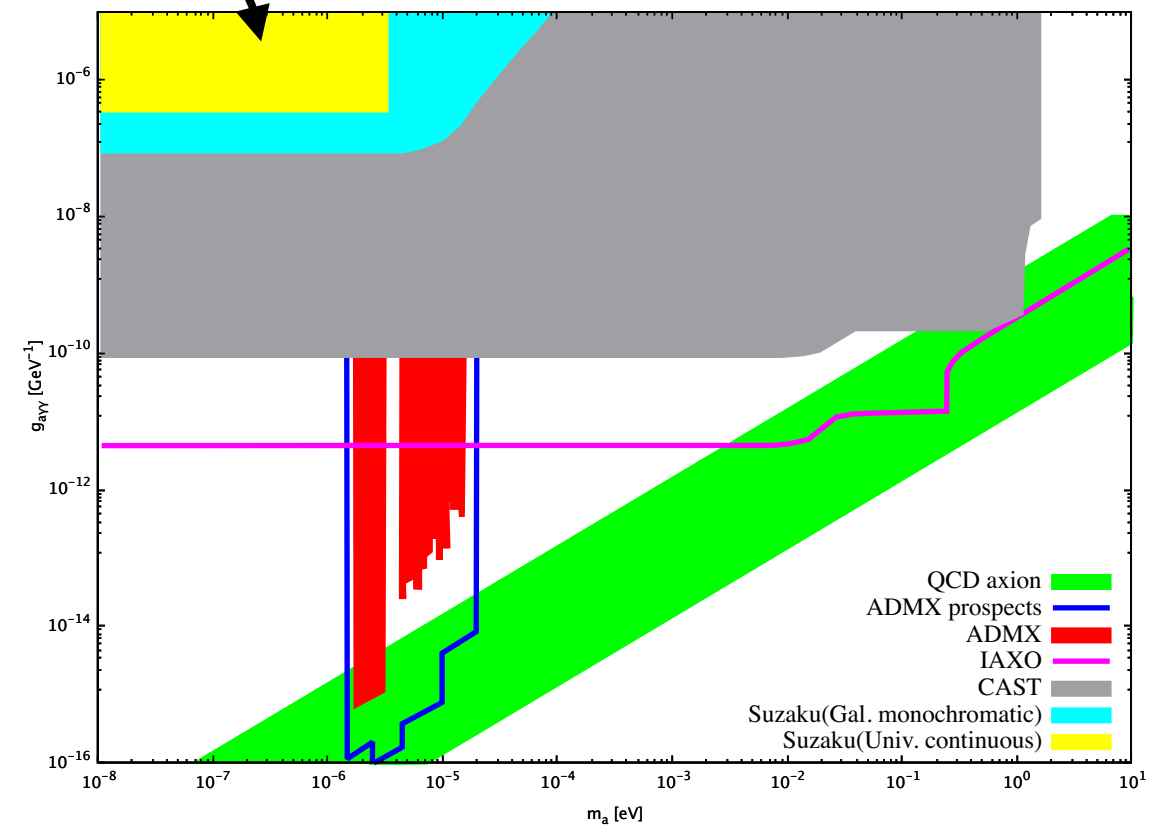


Upper limit of $\propto (B_{\perp}L)^2 E^{0.5}$ emission

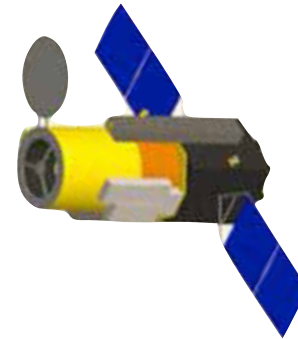
Four blank sky directions



with assumptions of dark matter mass, density & decay rate (somewhat unusual assumptions)



The best target is solar axion



Staying in the sun shade (at L2), no power generation from solar cells



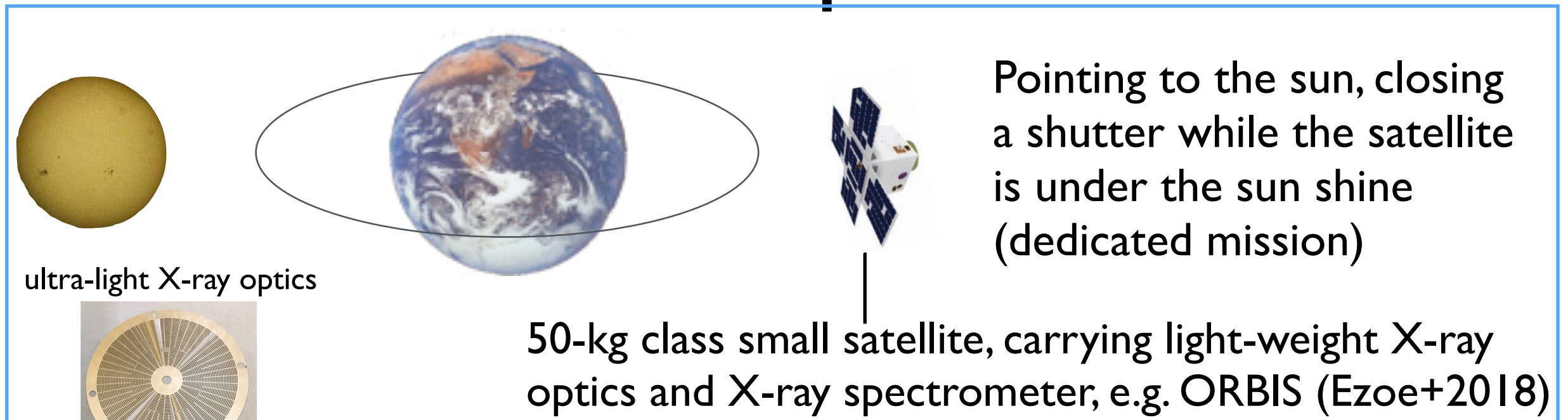
Pointing to the sun only while the satellite is in the sun shade, requires attitude maneuvers.



Pointing to the sun, closing a shutter while the satellite is under the sun shine (dedicated mission)

50-kg class small satellite, carrying light-weight X-ray optics and X-ray spectrometer, e.g. ORBIS (Ezoe+2018)

A solar-axion space mission

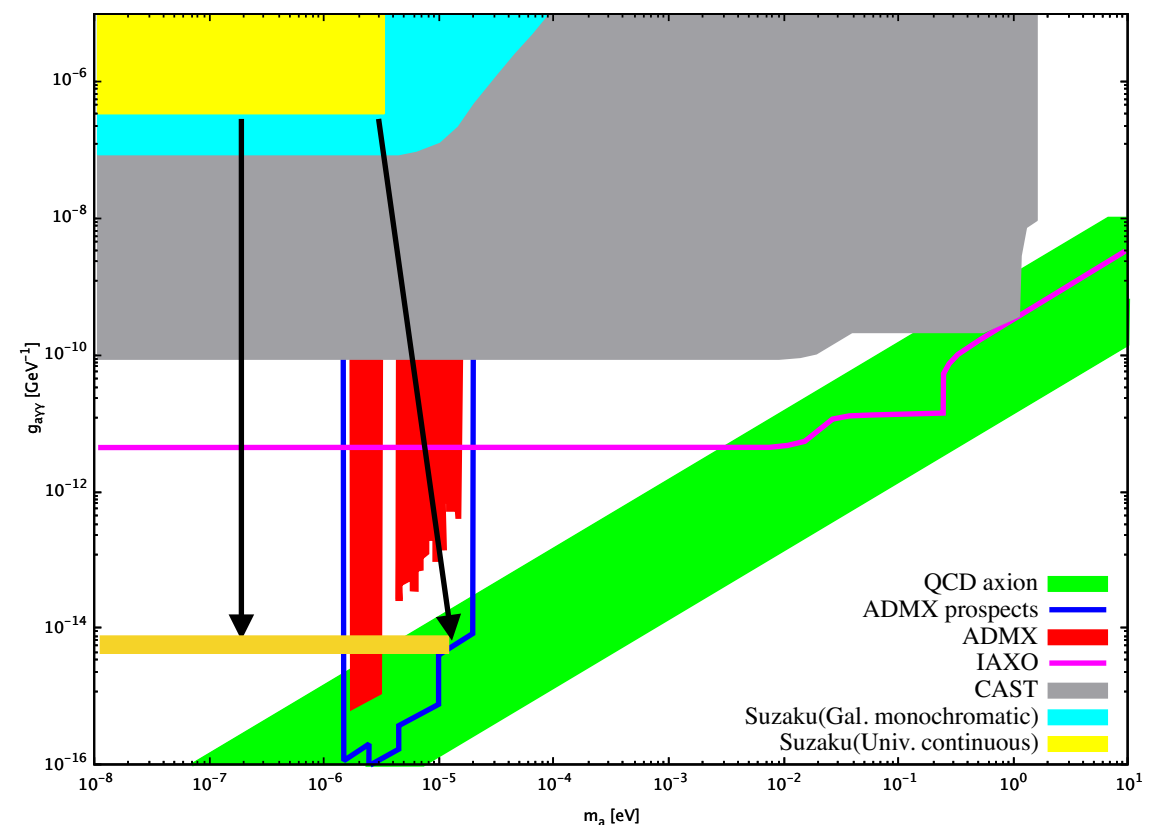


Advantages over Suzaku results

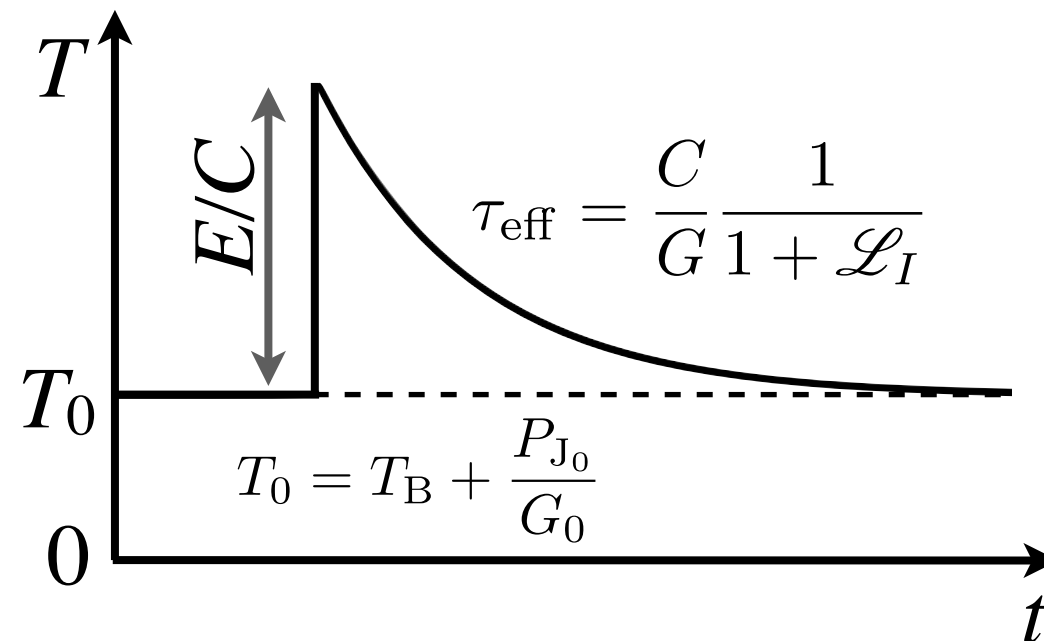
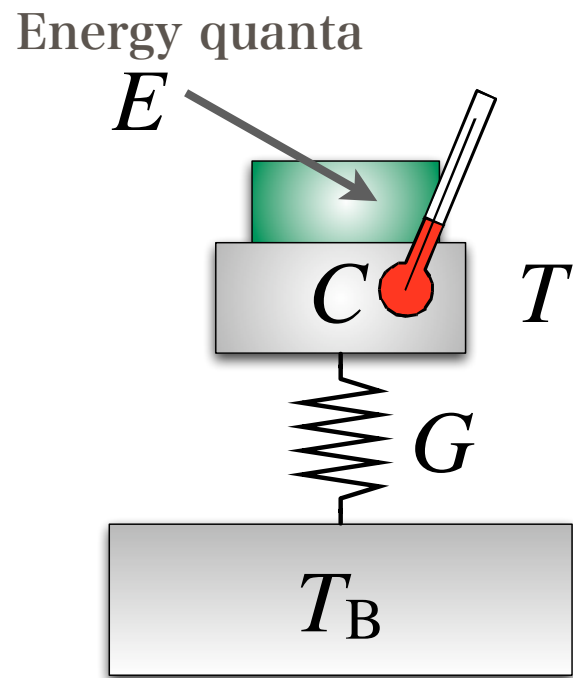
- higher source flux
- longer exposure (~ 5 days = a Suzaku obs. of single direction)
- background subtraction by image

Disadvantages

- Shorter L ($\sim 6 \times 10^3$ km, smaller BL)
 - less sensitivity but wider mass range
- smaller collecting area by a factor of ~ 10



Microcalorimeters



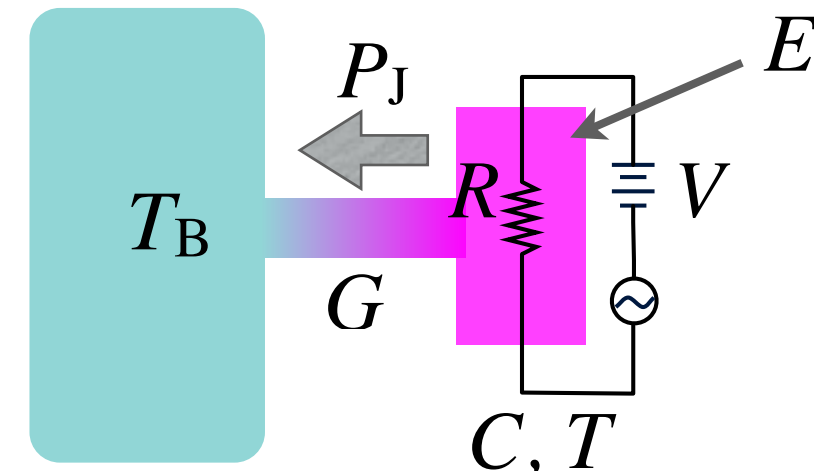
- Sensitive to any energy input → DM
- High energy resolution

$$\text{FWHM } \Delta E = 2.35\xi \sqrt{k_B T^2 C}$$

X-ray absorber of a few 100 μm square x a few μm thickness : $C \sim 1\text{pJ/K}@100\text{mK}$

$$\Rightarrow \Delta E = 5.4\xi \text{ eV} \quad \xi \sim 1$$

ETF (Electro-thermal feedback)



$$\mathcal{L}_I \equiv \frac{P_{J_0} \alpha_I}{G T_0} \sim \frac{\alpha_I}{n}$$

This figure is for
 $\alpha \equiv \frac{d \ln R}{d \ln T} > 0$. ETF
 works for $\alpha < 0$.

Towards large-format arrays

Thermometer	Si thermistor	TES	TES
Signal MUX	none	FDM/TDM/CDM	Microwave FDM
max possible # pixels in space	~100	a few k	~ 1M
Space mission	ASTRO-H SXS XRISM	Athena X-IFU	S-DIOS
# pixels	36	3168	~ 300 k
Launch year	2016/2021	2032	203X

Ground application: HOLMES (Nucciotti+2018)

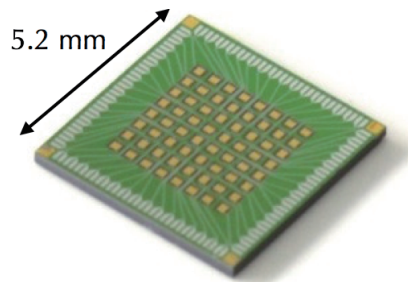
- End point spectrum of ^{163}Ho EC decay to constrain neutrino mass,
- 1024 TES microcalorimeters with microwave FDM readout

TES ground applications of our group

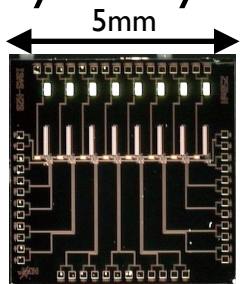
both utilize TES+DC readout

STEM TES EDX

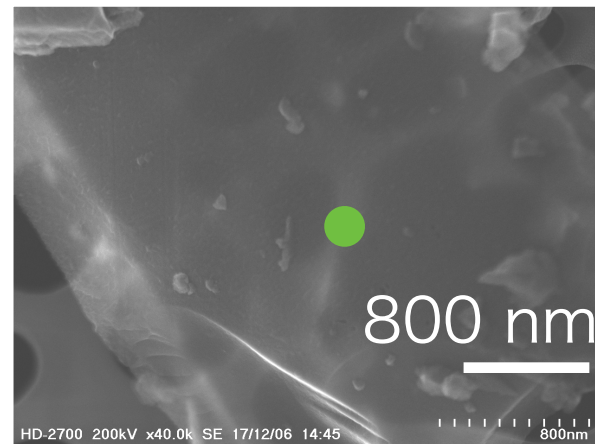
8x8 TES array



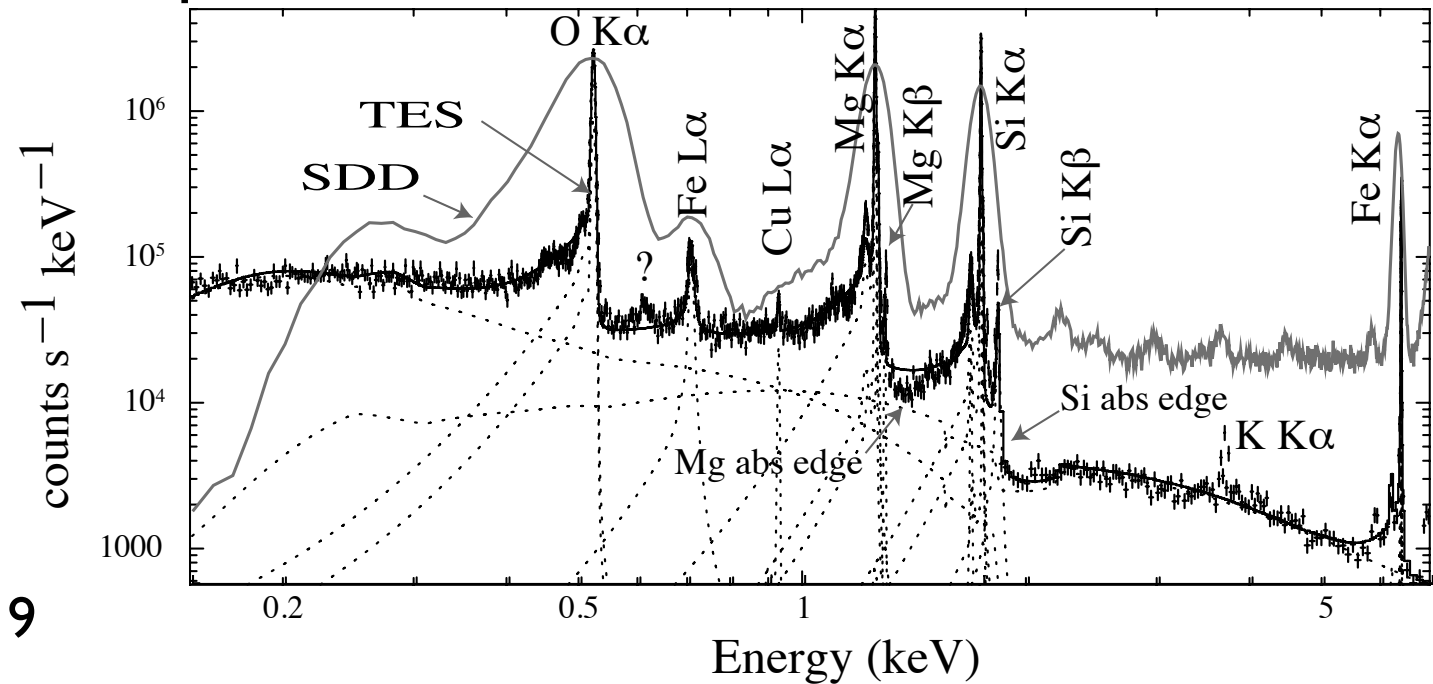
15 series SQUID array Array X 8



Olivin TEM image & EDX spectrum

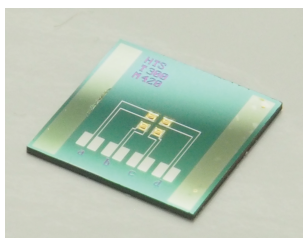


Hayashi 2018, Hayashi+2019

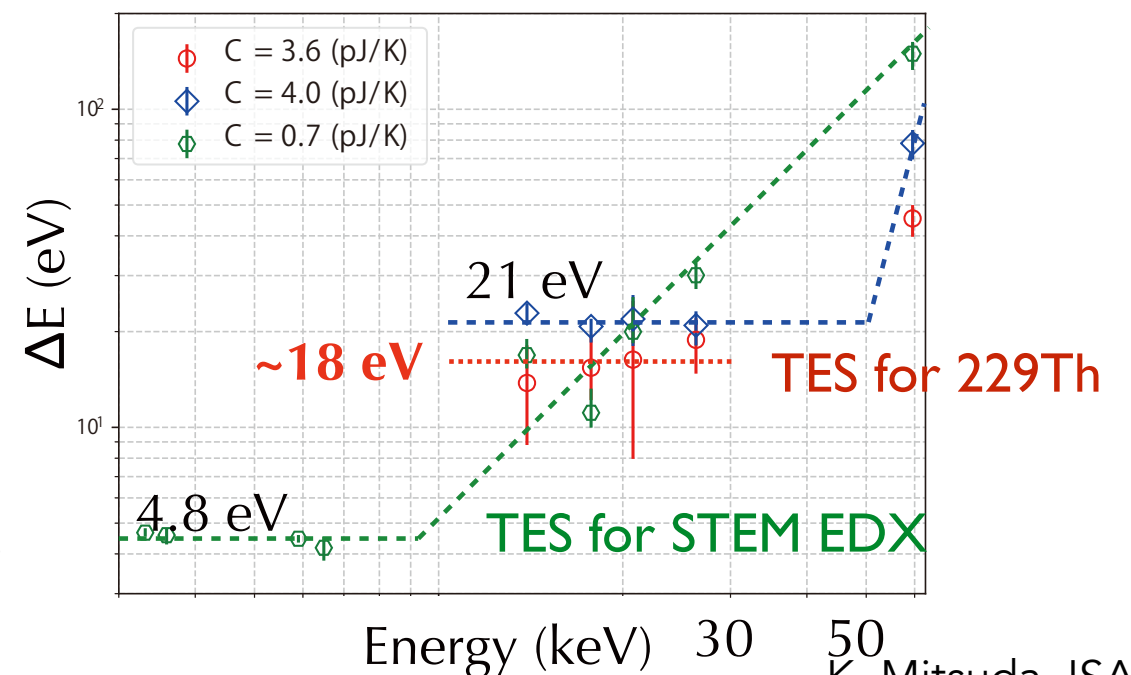


²²⁹Th experiment

TES microcalorimeter array & Detector head with SQUID array amp.



Muramatsu 2019



TES-microcalorimeter fabrication

All in-house process mostly using JAXA facilities

(a)



TES membrane sputtering

Tokyo Metro. Univ.

(b)



Photo mask alignment

(c)



Wet etching

(d)



Dry etching (ICP, DRIE)

JAXA nano clean room (Building D, Sagamihara)

(e)



Al sputtering deposition

(f)



EB vapor deposition

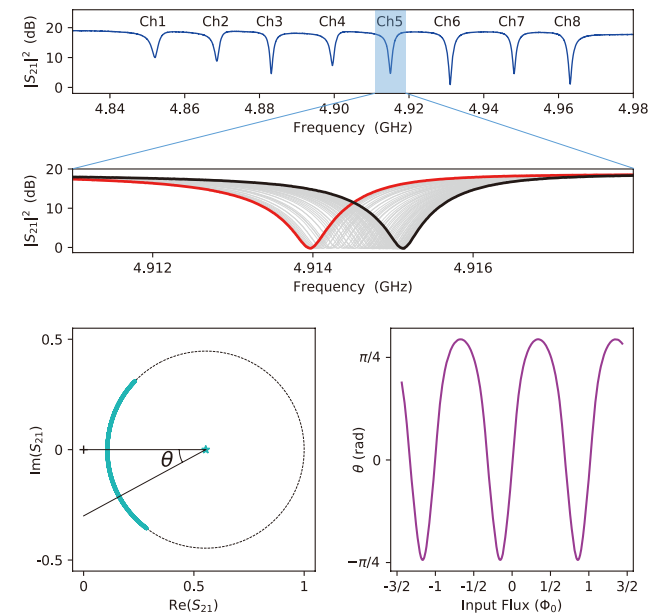
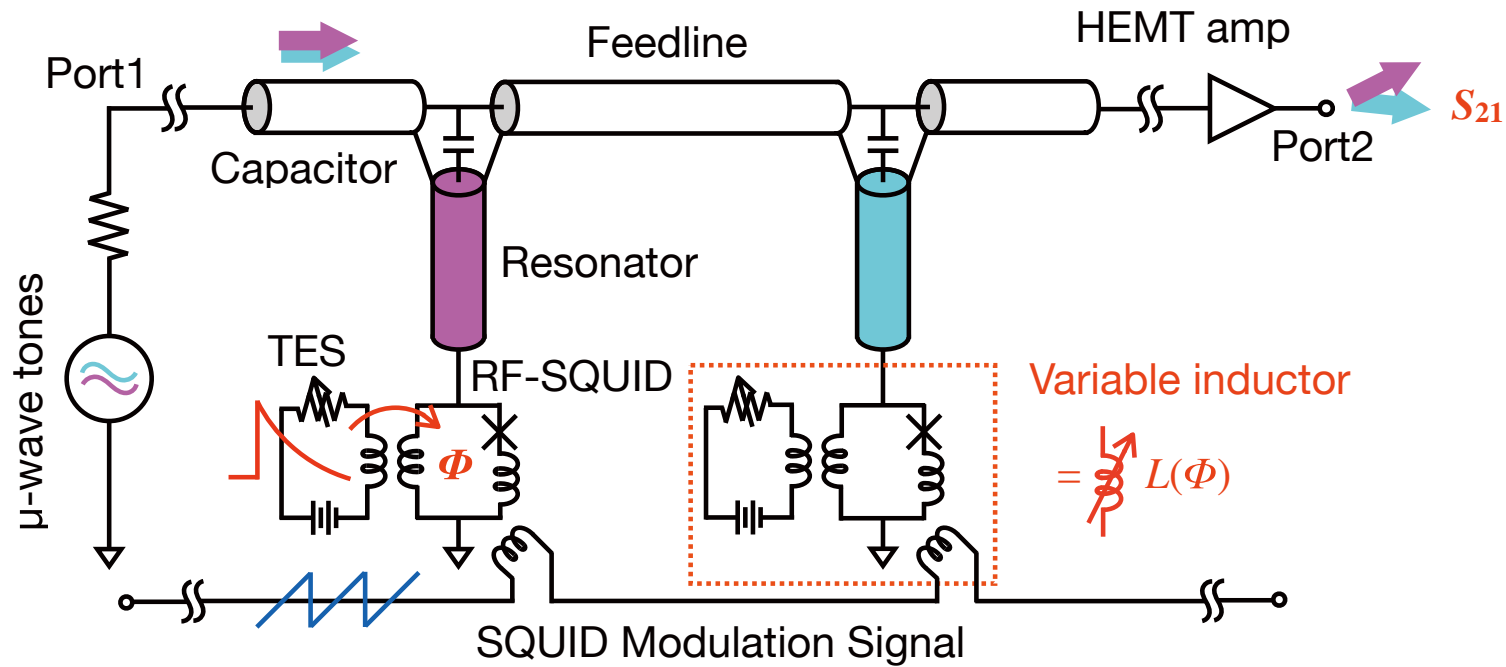
Mitsuda/Yamasaki laboratory clean booth
(Building A, Sagamihara)

Cryogenic readout electronics (SQUID array amplifiers) in the previous page were designed by our group and fabricated by CRAVITY of AIST

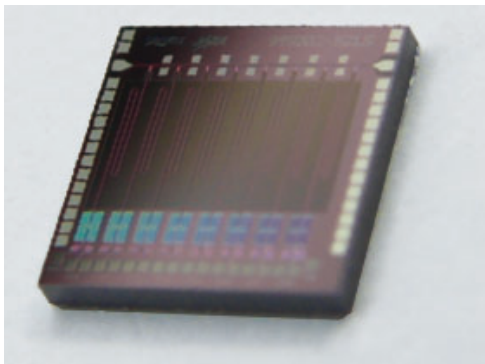
(Sakai+, IEEE 2015)

Microwave FDM development

collaboration with AIST



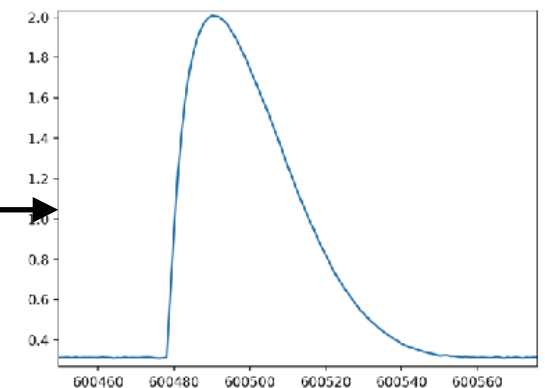
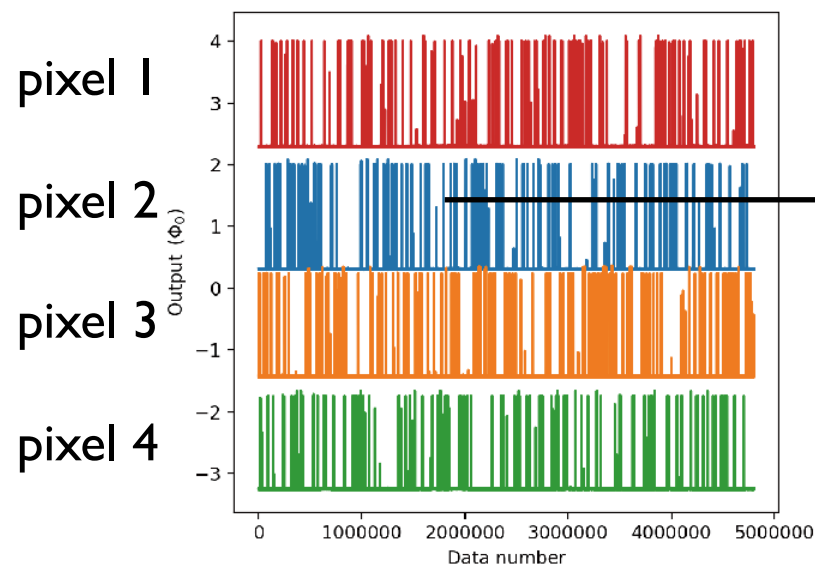
MUX chip
fabricated at CRAVITY of AIST



64 pix/ch MUX is expected
be realized soon

Kohjiro+2017
Nakashima+2018

example of de-MUXed signal



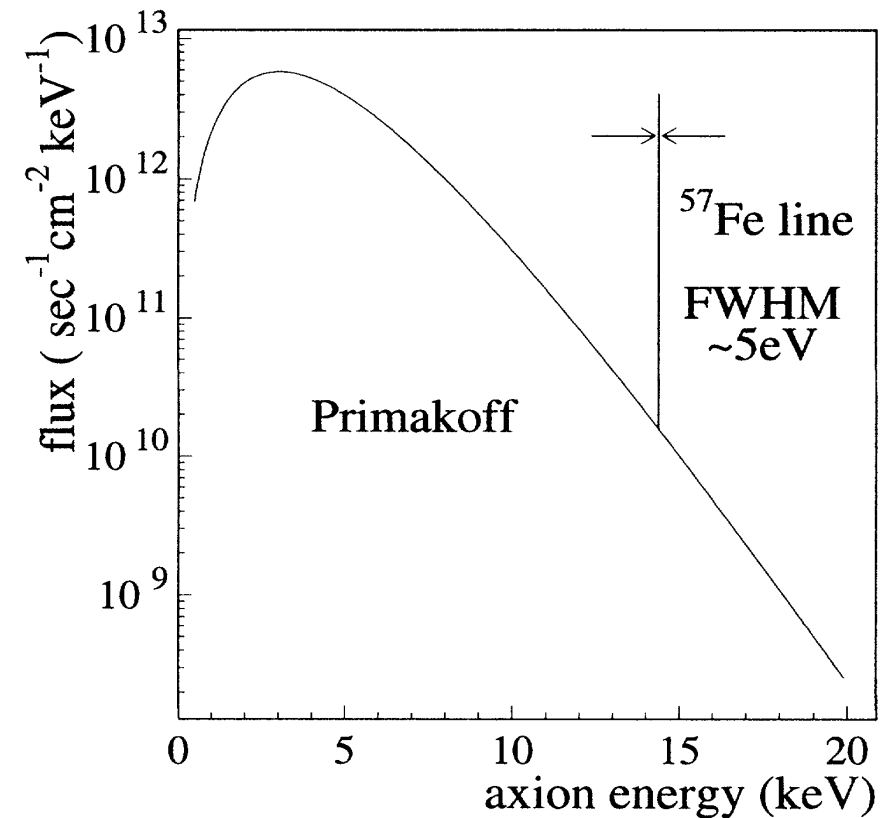
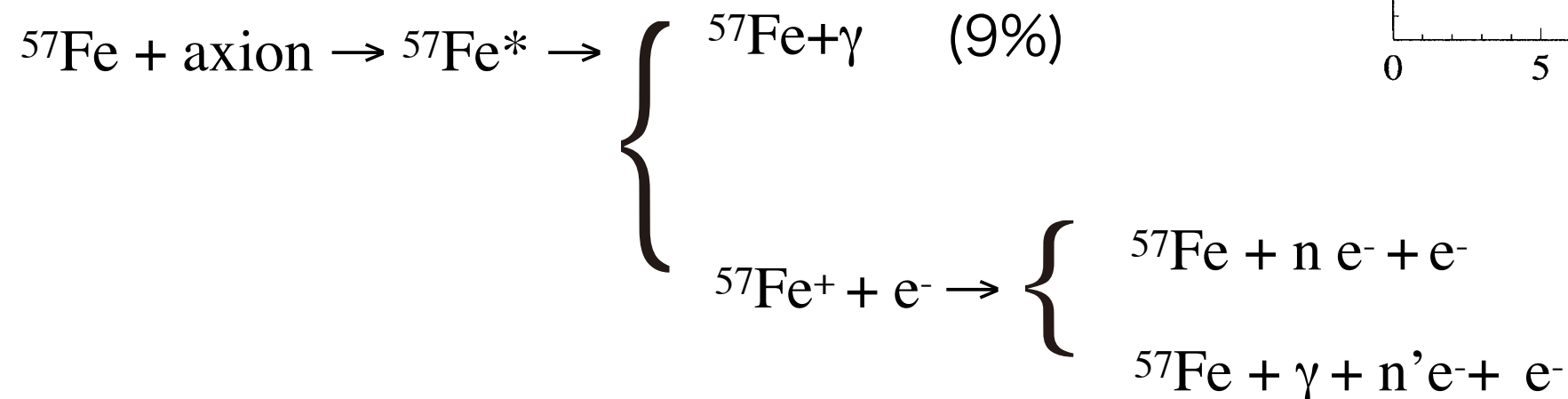
Search for monochromatic Solar axions

- Monochromatic axion emission predicted by Moriyama (1995)
- Semiconductor experiments by Namba (2007) and others.

Center of the sun:



Detector on ground:



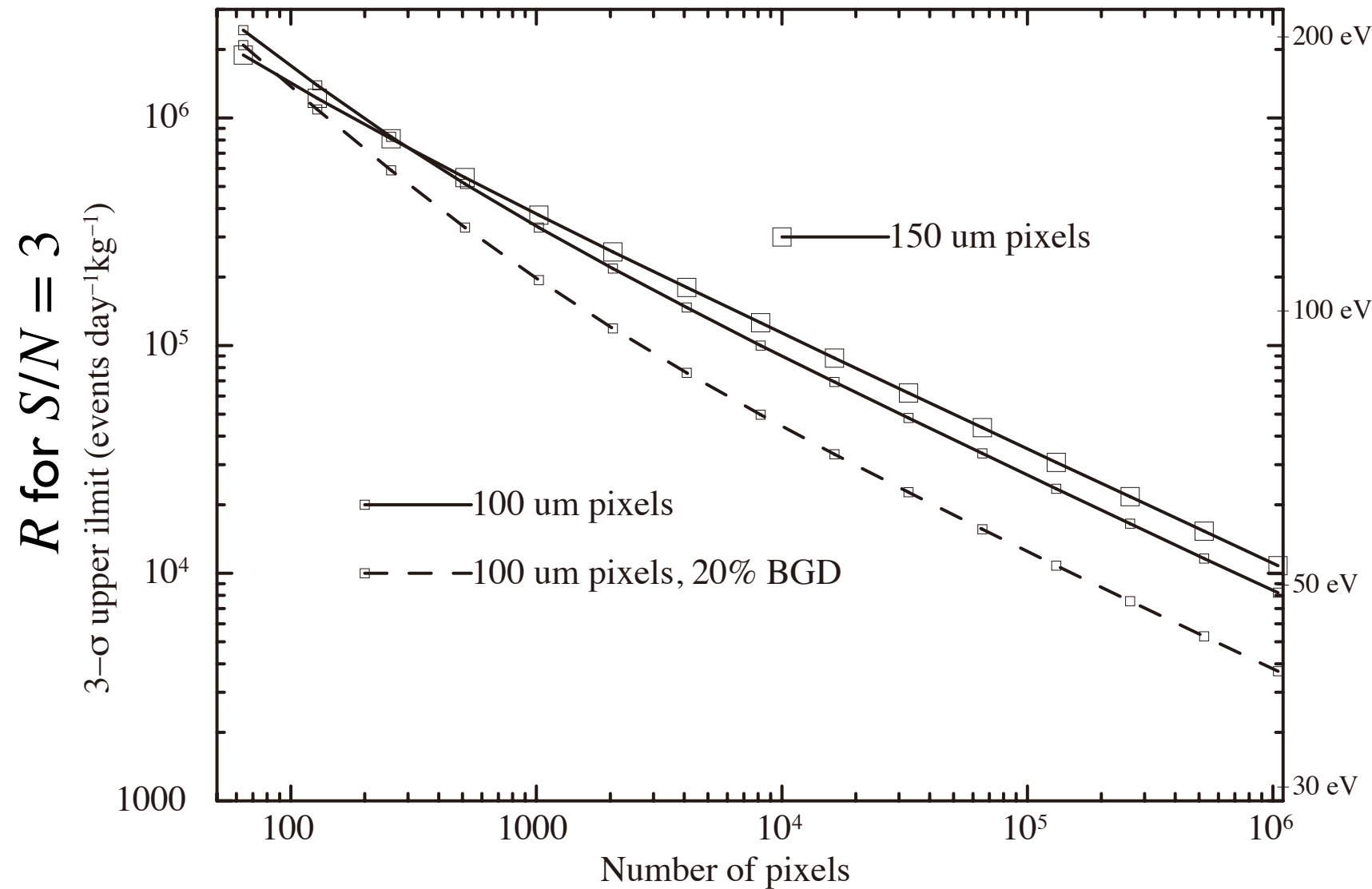
Moriyama (1995)

Search for monochromatic Solar axions

Microcalorimeter

- pros
 - Better efficiency because microcalorimeters are sensitive to conversion electrons and low energy X-rays. (~95%)
 - Sensitivity will be limited by signal Poisson fluctuation rather than background fluctuation because of good energy resolution (~10eV@14.4keV)
 - Axion converter mass can be increased by utilizing a large format array with microwave FDM readout.
- cons
 - TES performance will degrade with magnetic fields from the converter material, ^{57}Fe .
 - Yet small converter mass

Sensitivity prediction



Maehisa 2017

Assumptions

$$S/N = \frac{S}{\sqrt{S + b\Delta E\eta}}$$

S : total signal events

b : background events/eV

ΔE : energy resolution

η : fudge factor = 2.5

$$S = RTM\alpha$$

R : event rate

T : integration time

M : converter mass

α : detection efficiency

b : estimated from experiments

without anti-co

with anti-co (20% of above)

ΔE : pulse height position dependency
 assuming Fe thermal conductance in
 literature at low temperature

$$\Delta E = 7 \text{ eV} \left(\frac{L}{100\mu\text{m}} \right) \sqrt{1 + \left(\frac{L}{100\mu\text{m}} \right)^6}$$

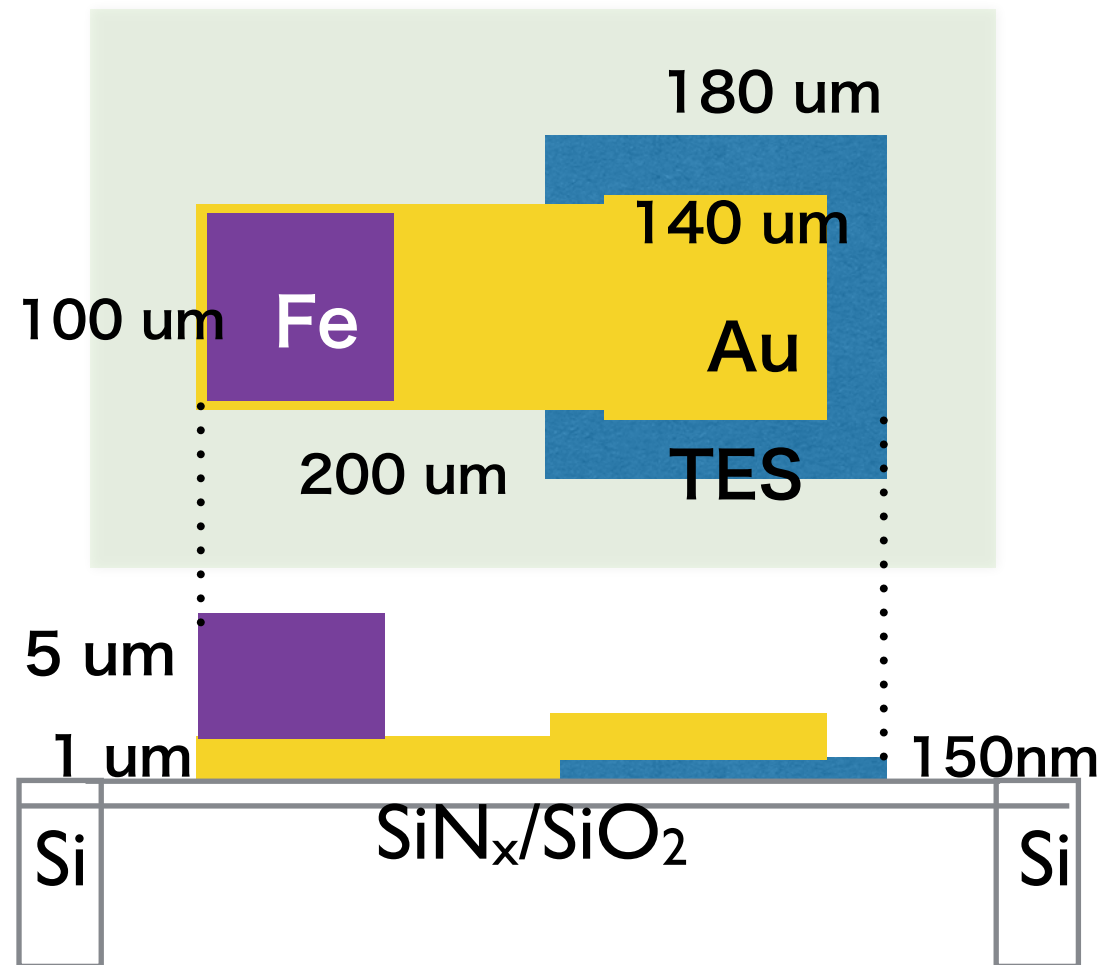
L : one side length of converter

TES design and development status

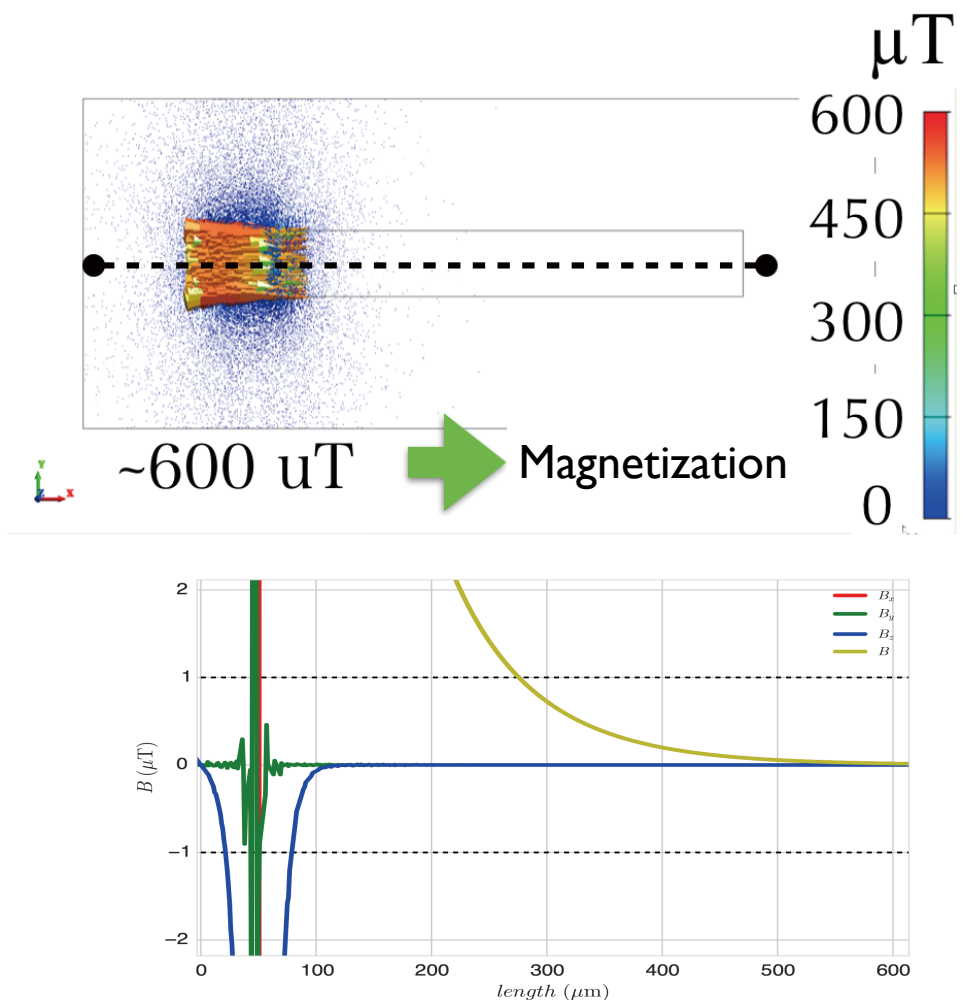
What we have done so far.

- | | order |
|---|-----------------------------------|
| • Design | |
| • Thermal strap was introduced to avoid magnetic field | 1 |
| • Thermal simulations with different strap lengths | 4 |
| • Iron membrane fabrication process | |
| • High-yield converter deposition process | 2 |
| • Electro deposition was selected and tested | ← collaboration with Waseda Univ. |
| • Material properties at low temperature | |
| • Thermal conductance of iron | |
| • Measurement of low temperature electrical conductance of iron membrane made by electro deposition. Then Wiederman-Frantz law applied. | 3 |
| • Degradation of TES due to magnetic field from iron | |
| • Magnetic field was estimated by using electro-magnetic field simulations | 3 |
| • R-T measurements of TES with and iron converter | 5 ← we are here now |

Concept design of a pixel

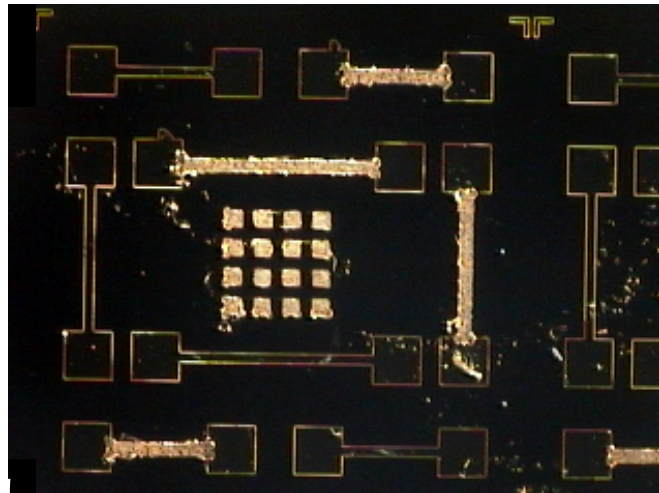


Example of magnetic field simulations



Condition: $B_{\perp} < 1 \mu\text{T}$ at TES

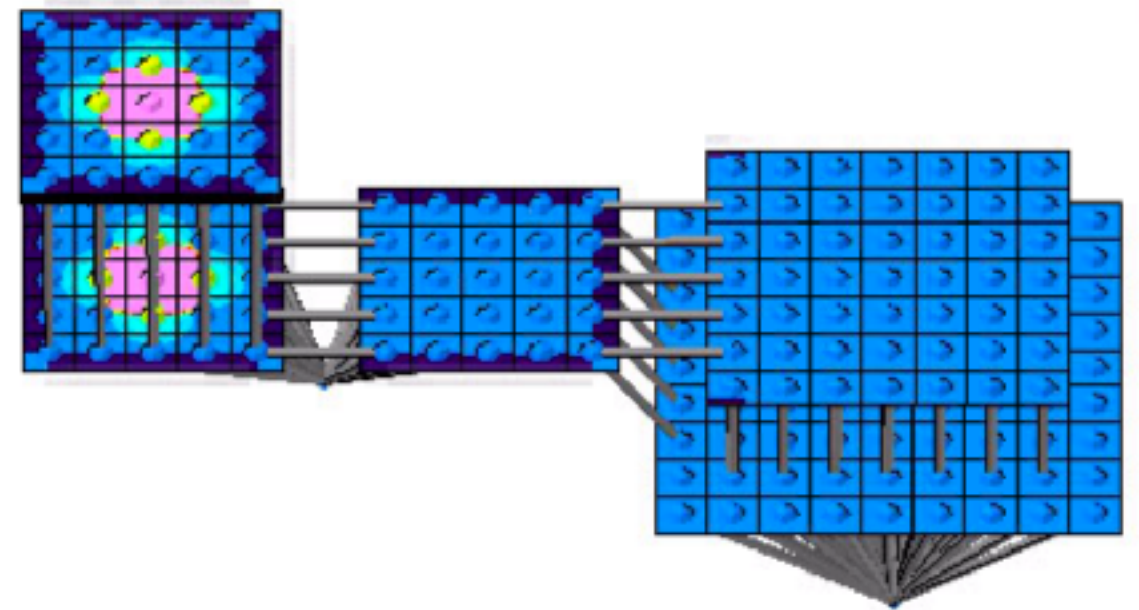
Thermal conductance measurement



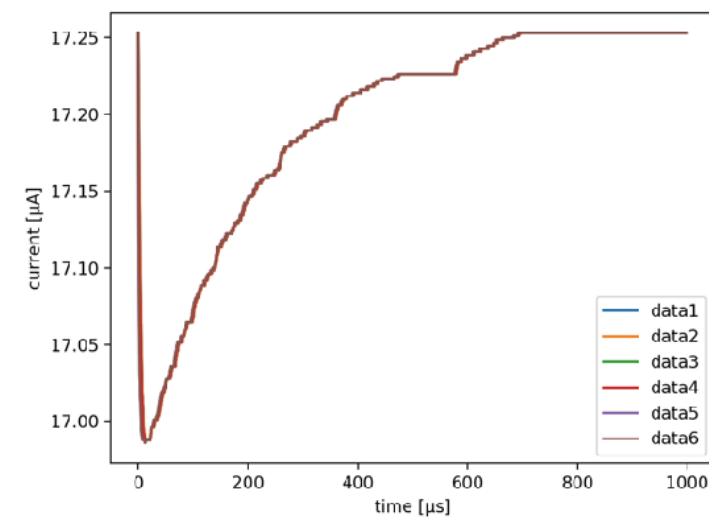
Iron membranes deposited and patterned on Si substrate.
(collaboration with Homma group at Waseda university)

Electrical conductance was measured at low temperature. Then the Wiedemann–Franz was applied to estimate thermal conductance.

FEM simulations of TES response



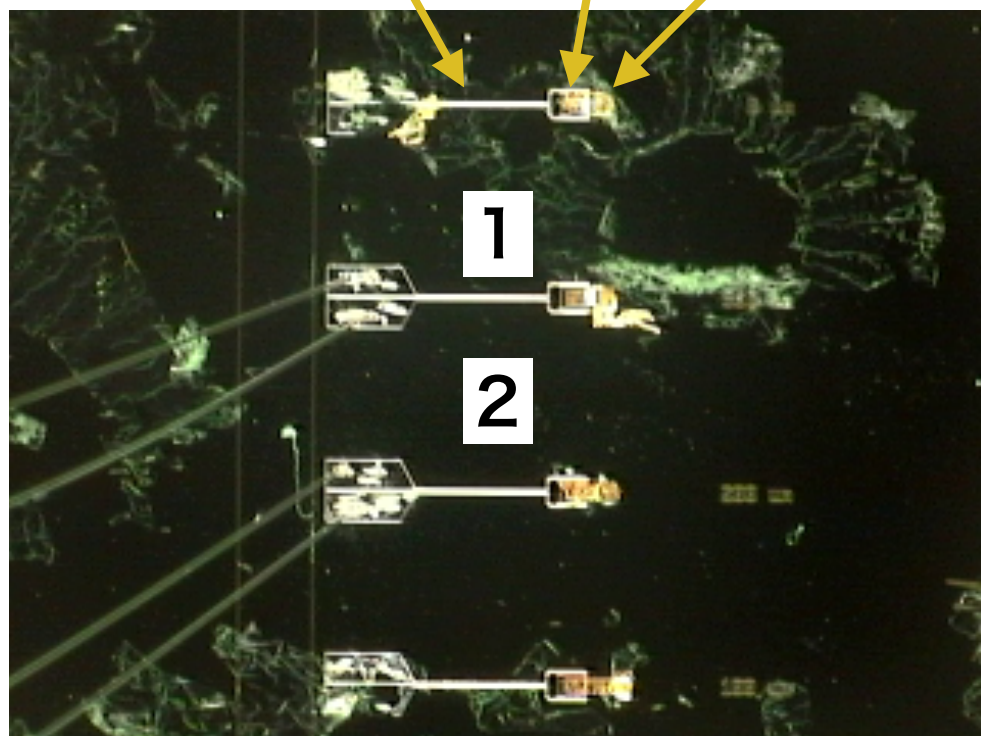
Position sensitivity to TES response was studied.



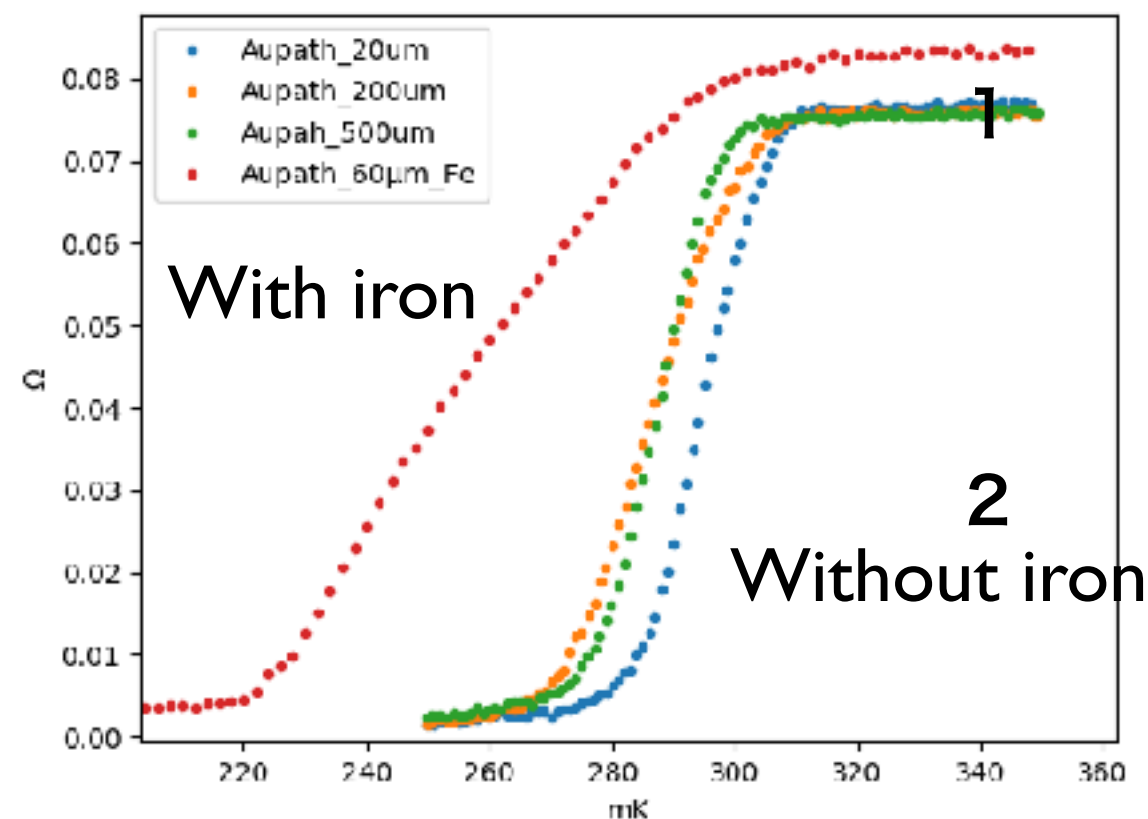
Degradation of $\Delta E < 5$ eV

Resistance-Temperature relation of TES

electrodes TES iron



green parts: lift-off
photo resist was not
removed perfectly.



Superconducting phase transition is affected by iron!
We need to make the distance larger.

I talked about

- Story of the 3.5 keV line, and astronomical searches of keV dark matter
 - Sterile neutrinos
 - Where to observe?
 - 3.5 keV line from clusters of galaxies
 - XMM-Newton (and Chandra) results
 - Suzaku results
 - ASTRO-H SXS results
 - Emission from the Milky-way halo by Suzaku
- Axion and ALP search using the earth's magnetic field
- Monochromatic solar-axion search
 - TES microcalorimeter development and ground applications
 - Signal multiplexing (MUX) for large format TES
 - TES microcalorimeter for solar-axion search